Comparative osteology of the fossorial frogs of the genus Synapturanus (Anura, Microhylidae) with the description of three new species from the Eastern Guiana Shield

Antoine Fouquet, Killian Leblanc, Anne-Claire Fabre, Miguel Rodrigues, Marcelo Menin, Elodie A Courtois, Maël Dewynter, Monique Hölting, Raffael Ernst, Pedro Peloso, et al.

Contents lists available at ScienceDirect

Zoologischer Anzeiger - A Journal of Comparative Zoology

journal homepage: http://ees.elsevier.com

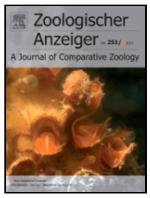

Research paper

Comparative osteology of the fossorial frogs of the genus *Synapturanus* (Anura, Microhylidae) with the description of three new species from the Eastern Guiana Shield

Antoine Fouquet [a,*], Killian Leblanc [a], Anne-Claire Fabre [b], Miguel T. Rodrigues [c], Marcelo Menin [d,1], Elodie A. Courtois [e], Maël Dewynter [f], Monique Hölting [g,h], Raffael Ernst [h], Pedro Peloso [i], Philippe J.R. Kok [b,j]

[a] *Laboratoire Evolution et Diversité Biologique, UMR 5174, CNRS, IRD, Université Paul Sabatier, Bâtiment 4R1 31062 Cedex 9, 118 Route de Narbonne, 31077, Toulouse, France*
[b] *Department of Life Sciences, The Natural History Museum, London, SW7 5BD, United Kingdom*
[c] *Universidade de São Paulo Instituto de Biociências, Departamento de Zoologia, São Paulo, SP, Brazil*
[d] *Departamento de Biologia, Instituto de Ciências Biológicas, Universidade Federal do Amazonas, 69080-900, Manaus, AM, Brazil*
[e] *LEEISA, Centre de Recherche de Montabo – IRD, 275 Route de Montabo, BP 70620, 97 334, Cayenne, French Guiana*
[f] *La Désirée, F-97351, Matoury, French Guiana*
[g] *Zoological Research Museum Alexander Koenig, Leibniz Institute for Animal Biodiversity, Adenauerallee 160, 53113, Bonn, Germany*
[h] *Museum of Zoology, Senckenberg Natural History Collections Dresden, Dresden, Germany*
[i] *Universidade Federal do Pará, Instituto de Ciências Biológicas, R. Augusto Corrêa, 1, Guamá, Belém, 66075-110, Pará, Brazil*
[j] *Department of Ecology and Vertebrate Zoology, Faculty of Biology and Environmental Protection, University of Łódź, 12/16 Banacha Str, Łódź, 90-237, Poland*

ARTICLE INFO

Article history:
Received 6 February 2021
Received in revised form 23 April 2021
Accepted 10 May 2021
Available online xxx
Corresponding Editor: Dr. Alexander Kupfer

Keywords
Amazonia
Amphibia
Integrative taxonomy
Morphology
Tomography

ABSTRACT

The genus *Synapturanus* includes three nominal species of fossorial Amazonian frogs. A previous study combining molecular, morphological and acoustic data suggested that there may be six times more species than currently recognized. Herein we describe and name three of these new species and compare their osteology. *Synapturanus zombie* sp. nov. occurs in French Guiana and Amapá (Brazil), *Synapturanus mesomorphus* sp. nov. in Guyana and adjacent Venezuela, and *Synapturanus ajuricaba* sp. nov. in the northern part of the Brazilian states of Amazonas and Pará. These species are readily differentiated from congeners by a combination of external morphological characters such as body size, development of fringes on fingers and coloration, by advertisement call variables, and by osteological traits. Along with osteological reinforcement of the skull, atlas and scapular region, the reduction of the size of phalanges, more developed fringes on fingers, smaller eyes and larger body size, altogether suggest an overall increase of the fossorial habits in the easternmost species. In contrast, the relatively conserved morphology of the posterior part of the body across the genus suggests that fossoriality mostly involves the anterior part. Furthermore, the fusion of tarsal bones in the species of the western clade may indicate locomotory adaptation to more epigean habits.

1. Introduction

Microhylidae is one of the largest family of amphibians, with a global distribution and a remarkable diversity of morphological and ecological traits. Within the Neotropics, microhylids represent 18% of the total number of described species (Frost, 2021) and belong to two major groups: Gastrophryninae Fitzinger, 1843, the most species rich subfamily with 81 species (Frost, 2021) distributed from southern North America to Argentina; and a species poor clade formed by the monotypic Adelastinae Peloso, Frost, Richards, Rodrigues, Donnellan, Matsui, Raxworthy, Biju, Lemmon, Lemmon, and Wheeler, 2016 and Otophryninae Wassersug & Pyburn, 1987. The latter subfamily is limited to two genera, each including three valid nominal species: *Otophryne* Boulenger, 1900 and *Synapturanus* Carvalho, 1954, all described from the Guiana Shield. Whereas *Otophryne* are epigean, diurnal, and ripicolous species with exotrophic tadpoles, *Synapturanus* are fossorial, nocturnal, associated with well drained soils of *terra-firme* (non-flooded) forests and have an endotrophic mode of development (Pyburn, 1975; Menin et al., 2007). The three known species of *Synapturanus* (*Synapturanus mirandaribeiroi* Nelson & Lescure, 1975, *Synapturanus rabus* Pyburn, 1977, and *Synapturanus salseri* Pyburn, 1975), occur in the lowlands and seemingly have very brief and rare periods of calling activity (Nelson & Lescure, 1975; Ernst et al., 2005). Individuals have been observed in underground galleries and nuptial chambers, which they dig to deposit eggs that un-

* Corresponding author.
E-mail address: fouquet.antoine@gmail.com (A. Fouquet)
[1] Deceased.

https://doi.org/10.1016/j.jcz.2021.05.003
0044-5231/

dergo endotrophic development (Nelson & Lescure, 1975; Pyburn, 1975; 1977; Menin et al., 2007). Although no direct observations have been reported, the overall morphology, and notably the shape of the snout and humerus, suggest a head-first, forward-burrowing, behavior (Keeffe & Blackburn, 2020; Fouquet et al., 2021). Overall, *Synapturanus* are poorly known, and the scarcity of basic data on their life-history and rarity in zoological collections is easily explained by their secretive lifestyle.

Using a combination of genetic, acoustic and morphological data, Fouquet et al., 2021 demonstrated that the diversity in Otophryninae is largely underestimated. For *Synapturanus*, for example, the study suggests that at least another 15 species could be formally recognized. Such an underestimation of the species diversity in *Synapturanus* is partly explained by the combination of (1) the difficulty to access many remote parts of Amazonia; (2) the challenging task that collecting these markedly fossorial and secretive species represents; (3) the scarcity of comprehensive acoustic, molecular and morphological reference data, especially from topotypical material, rendering comparison and description difficult; and (4) the prevalence of small and allopatric distributions of the different species probably linked to low dispersal ability and specific ecological requirements.

The phylogenetic data in Fouquet et al., 2021 also demonstrated that three major clades exist within *Synapturanus*. *S. salseri*, *S. mirandaribeiroi* and seven additional candidate species form a clade occurring in the Guiana Shield as well as extending into the southern part of the Amazon River basin. *S. rabus* and six candidate species belong to a clade restricted to western Amazonia. The third clade is formed by two unnamed candidate species from central Amazonia. *S. mirandaribeiroi* was described based on specimens from Kanashen (also spelled "Konashen", Southern Guyana) and was reported throughout the Guiana Shield (Nelson & Lescure, 1975; Pyburn, 1975; Lima et al., 2006; Menin et al., 2007; Ávila-Pires et al., 2010; Barrio-Amorós et al., 2019), as well as the right bank of the Rio Negro, in the Jaú National Park (Neckel-Oliveira & Gordo, 2004). However, genetic, morphological and acoustic variation across this range suggests that some of these populations may not belong to *S. mirandaribeiroi*. The similarity between the skull and humerus of the paratype (MNHN-RA-1974.0397) and that of specimens from southwestern French Guiana, Suriname and the Manaus region, an area encompassing the type locality of *S. mirandaribeiroi*, strongly suggests conspecificity (Fouquet et al., 2021). Moreover, genetic data indicate that these specimens form a lineage related to populations located in the southern part of the Amazon River basin (*Synapturanus* sp. "Purus" and *Synapturanus* sp. "Tapajos") that are phenotypically distinct. However, they are also related to a single specimen (*Synapturanus* sp. "Taboca") that is genetically albeit not morphologically distinct from *S. mirandaribeiroi*. This specimen is from a locality (Taboca, Amazonas, Brazil) also relatively close to Kanashen (ca. 310 km airline). Therefore, some ambiguity remains whether all these populations belong to a single species, i.e., *S. mirandaribeiroi*, or if the name *S. mirandaribeiroi* only applies to one of these two groups of populations (Fouquet et al., 2021).

S. salseri was described from Vaupés, Colombia, and populations from Brazil's Manaus region (Lima et al., 2006; Menin et al., 2007), Venezuela (Barrio-Amorós et al., 2019), and Guyana (Kok & Kalamandeen, 2008) have also been tentatively assigned to this taxon. Unfortunately, no DNA sequences unequivocally assignable to this taxon (i.e., from the type locality or its vicinity) have been made available yet (Peloso et al., 2016 included sequences labeled as "*S. salseri*", but these sequences belong to one of the unnamed candidate species of Fouquet et al., 2021). Furthermore, the morphology of the skull and of the humerus suggest that this name cannot be applied to any known populations outside of the type locality (Fouquet et al., 2021).

Finally, *S. rabus* belongs to a clade formed by species from western Amazonia displaying distinct calls (short notes) and morphology (elongated body and limbs) (Fouquet et al., 2021).

Herein, we describe and name three of these new species, previously reported as *Synapturanus* sp. "Eastern Guianas", *Synapturanus* sp. "Guyana" and *Synapturanus* sp. "Manaus" (Fouquet et al., 2021), for which we could gather sufficient phylogenetic, morphological (external and osteology) and acoustic evidence to diagnose the new taxa from currently valid nominal species.

2. Material and methods

2.1. External morphology

We examined 38 specimens of the new species (7 *S.* sp. "Eastern Guianas", 8 *S.* sp. "Manaus", 23 *S.* sp. "Guyana") deposited in various zoological collections (Appendix A), and compared them with specimens of the three named species of the genus, *S. mirandaribeiroi*, *S. salseri*, and *S. rabus*, including type specimens and topotypical material (Table 1, Appendix B). Among those specimens, 12 were included in the genetic dataset of Fouquet et al., 2021 and are thus directly linked to candidate species. The other specimens were assigned to one of the species based on morphological examination and on the geographic proximity of their collecting locality relative to that of a genotyped specimen.

We measured 12 morphological variables on examined specimens, following Kok & Kalamandeen (2008): snout-vent length (SVL); head length, from the corner of the mouth to the tip of the snout (HL); head width at the level of the angle of jaws (HW); eye-to-naris distance, from the anterior edge of the eye to the center of the naris (EN); internarial distance (IN); horizontal eye diameter (ED); interorbital distance, representing the width of the underlying frontoparietal (IO); forearm length, from the proximal edge of the palmar tubercle to the outer edge of the flexed elbow (FAL); hand length, from the proximal edge of the palmar tubercle to the tip of the Finger III (HAND); crus (tibiofibular) length, from the outer edge of the flexed knee to the heel (TL); foot length, from the proximal edge of the inner metatarsal tubercle to the tip of Toe IV (FL); and thigh length, from the vent opening to the outer edge of the flexed knee (ThL).

2.2. Bioacoustics

We compiled call recordings of 11 males of the new species (4 *S.* sp. "Eastern Guianas", 5 *S.* sp. "Manaus", 2 *S.* sp. "Guyana") from various available sources (see Fouquet et al., 2021), and compared them to the calls of *S. mirandaribeiroi*, *S. rabus* and *S. salseri*. We followed a call-centered approach and measured four call variables following those standardized in Köhler et al. (2017): Note Length (NL), Dominant Frequency (DoF, which also corresponds to the fundamental frequency in the genus; taken with a spectral slice over the entire note), Delta Frequency (DeF) (difference in peak frequency between spectral slices taken over the first and the last 0.015 s of the note), inter-note length (the silence between the end of one note and the beginning of the next one). We measured temporal and spectral variables from waveforms and spectrograms using Audacity v.2.4.1 (Audacity Team, 2020). These recordings are heterogeneous in terms of length and quality. Calls recorded with high quality are often single or in very low numbers per recording and we selected the ones with the best quality to measure acoustic variables. When more than one good quality call was available per recorded male, we used the average calculated across up to four measures.

Table 1
Morphological measurements in mm (individual measurements are available in Appendix D).

			SVL	HL	HW	IO	IN	EN	ED	FAL	HAND	ThL	TL	FL
S. mirandaribeiroi	M (n = 14)	Mean	29.1	5.7	6.1	3.7	1.9	2.0	1.5	4.4	4.9	10.7	10.8	10.9
		min	26.6	5.2	4.9	3.3	1.7	1.7	1.3	3.7	4.2	8.2	9.8	9.6
		max	30.8	6.5	6.5	4.0	2.1	2.2	1.7	4.9	5.6	12.4	12.2	11.9
	F (n = 3)	Mean	31.5	6.1	6.5	3.8	2.0	2.1	1.5	4.5	5.2	11.4	11.4	11.3
		min	28.6	5.9	5.8	3.4	1.9	2.0	1.3	3.6	4.5	10.5	10.3	10.3
		max	34.4	6.4	7.6	4.1	2.1	2.2	1.6	5.0	5.9	12.6	12.6	12.9
S. zombie sp. nov.	M (n = 5)	Mean	39.2	7.4	7.5	4.8	2.4	2.4	1.5	5.7	7.1	14.4	13.8	13.9
		min	37.0	7.3	7.2	4.4	2.2	2.0	1.4	5.1	6.8	13.7	13.1	13.5
		max	40.6	7.7	7.8	5.1	2.6	2.7	1.6	6.5	7.4	15.2	15.1	14.4
	F (n = 2)	Mean	40.5	7.0	7.7	4.7	2.5	2.5	1.6	5.7	7.0	13.5	13.6	13.5
		min	39.0	6.9	7.7	4.6	2.4	2.4	1.6	5.6	6.7	12.5	13.4	13.4
		max	42.1	7.1	7.7	4.9	2.5	2.6	1.7	5.9	7.2	14.4	13.8	13.5
S. mesomorphus sp. nov.	M (n = 4)	Mean	24.8	5.0	5.2	3.0	1.8	1.7	1.4	3.6	4.0	8.8	10.0	10.8
		min	23.0	4.8	5.1	2.9	1.7	1.6	1.3	3.3	3.8	8.3	9.1	9.4
		max	26.0	5.1	5.5	3.1	1.8	1.9	1.6	3.8	4.2	9.5	10.7	13.1
	F (n = 7)	Mean	28.0	5.5	5.6	3.3	1.8	1.8	1.5	4.0	4.7	9.7	11.3	10.9
		min	27.1	4.7	5.1	3.0	1.5	1.6	1.2	3.5	4.3	8.5	10.8	10.0
		max	29.4	6.3	6.5	3.7	1.9	2.1	1.6	4.5	4.9	10.7	11.8	11.6
S. ajuricaba sp. nov.	M (n = 5)	Mean	31.8	6.1	6.2	3.7	1.9	2.5	1.6	4.9	5.4	11.8	11.8	11.3
		min	29.3	5.9	5.8	3.5	1.8	2.3	1.6	4.7	5.2	11.1	10.8	10.6
		max	33.2	6.4	6.6	3.9	2.1	2.6	1.7	5.3	5.7	12.5	12.7	12.0
	F (n = 3)	Mean	36.5	6.3	7.0	4.3	2.5	2.5	1.7	5.7	5.8	12.1	12.2	11.7
		min	35.9	6.2	6.7	4.2	2.3	2.3	1.6	5.4	5.7	11.4	11.7	10.9
		max	37.3	6.5	7.3	4.3	2.6	2.6	1.7	6.0	5.9	12.6	12.7	12.4

2.3. Osteology

Fouquet et al., 2021 unraveled an extensive osteological (skull and humerus) variation among candidate species using morphometric data from micro computed tomography scans (μCT-scans). We expanded the study of this variation to the entire skeleton (skull, vertebral column, pectoral and pelvic girdles) of (1) the three new species (1 male and 1 female of each except in *S.* sp. "Manaus", for which only two females were available); (2) *S. mirandaribeiroi* (1 male paratopotype and 1 male and 1 female recently collected); (3) *S. salseri* (1 male paratopotype); (4) *S.* sp. "Ecuador", as a representative of the western clade (1 male and 1 female); and (5) *S.* sp. "Juami", as a representative of the central clade (1 male and 1 female). These μCT-scans were retrieved from www.morphosource.org (Appendix C). Fourteen specimens used for osteological comparisons were also genotyped and could thus be directly linked to the DNA-based species delimitation of Fouquet et al., 2021.

Osteological descriptions are based on surfaces rendered in AVIZO using the 'phong' renderer with a custom preset (available from the corresponding author upon request), adjusted for each scan to reveal the skeleton but not the rest of the matrix. Scans with edge and beam-hardening artefacts were refined using local thresholds, clipping planes with Geomagic. Anatomic figures were constructed using image captures with MeshLab function "snapshot" under an orthographic field of view. Measurements were taken from these models using MeshLab measuring tool (Fig. S1). Osteological terminology follows Trueb (1968, 1973), with that of the carpals and tarsals following Fabrezi & Alberch (1996). Newly obtained surface rendering of the scans are deposited at http://morphosource.org/Detail/ProjectDetail/Show/project_id/254. Readers are advised that micro-CT preparations are targeted to render osteology and do not render most of the cartilage. Therefore, as too few specimens were available for clearing and staining, we opted to omit cartilage descriptions from our skeletal descriptions and comparisons below.

3. Results

Herein, we formally describe and name three new species of *Synapturanus* previously recognized in Fouquet et al., 2021 as *Synapturanus* sp. "Eastern Guianas", *Synapturanus* sp. "Manaus" and *Synapturanus* sp. "Guyana". As the three new species are nested in the eastern clade of Fouquet et al., 2021, along with *S. salseri*, *S. mirandaribeiroi* and four additional putative new species, we rediagnose the first two species and comment upon relevant information before formally describing the new taxa.

3.1. Taxonomic accounts

Members of the genus *Synapturanus* are mainly characterized by the following external features: (1) body stout, usually globular; (2) snout long, strongly protruding, projecting well beyond the end of the lower jaw; (3) tympanum usually concealed and only distinct anteroventrally; (4) nares oriented laterally, closer to the tip of the snout than to the eye; (5) loreal region strongly concave, grooved; (6) supratympanic fold running from the posterior corner of the eye, curving towards the axilla; (7) occipital (postcephalic) fold continuous with supratympanic fold; (8) gular fold continuous with occipital fold; (9) presence of a thoracic fold; (10) skin on dorsum smooth; (11) skin on venter smooth;

(12) fingers short, relative length of fingers III > IV > II > I; (13) toes unwebbed, relative length of toes IV > III > V > II > I; (14) subarticular tubercles not visible on toes; (15) absence of vocal slits; (16) absence of vocal sac; (17) absence of maxillary teeth; and (18) glandular unpigmented supracarpal pad present in males (poorly visible in preservative).

3.1.1. Synapturanus mirandaribeiroi Nelson & Lescure, 1975

3.1.1.1. Holotype MZUSP49981 an adult female collected by Craig E. Nelson and Gene A. Miller between the 17th and the 30th of July 1968 at Kanashen (a Waiwai Indian village and mission) on the Upper Essequibo River, Rupununi District, Guyana.

3.1.1.2. Allotype AMNH90935, an adult male with the same data as the holotype.

3.1.1.3. Paratypes A series of six males, five females, and two juveniles with the same data as the holotype, deposited as follows: AMNH90936–90943, MNHN-RA-1974.0397, National Museum of Guyana (numbers not mentioned by Nelson & Lescure, 1975), and UMMZ136147.

3.1.1.4. Material examined MZUSP49981, AMNH90935, AMNH90937, MNHN-RA-1974.0397 and the following 16 non type specimens referred to as *S. mirandaribeiroi*: MNHN-RA-2020.0079–82, INPA-H10890, INPA-H11837, INPA-H11843, INPA-H11867, INPA-H13169–70, INPA-H18572, INPA-H19781, INPA-H34023, INPA-H37891 (Appendix B).

3.1.1.5. Definition and diagnosis (1) Medium-sized *Synapturanus* (average male SVL 29.1 mm [26.2–30.8, n = 14], female SVL 31.5 mm [28.6–34.4, n = 3]) (Fig. 1; Table 1); (2) head dorsally convex in lateral view; (3) eyes small, slightly smaller than eye-naris distance; (4) fingertips rounded; (5) subarticular tubercles not visible on fingers; (6) thenar tubercle large and prominent, palmar tubercle indistinct; (7) Fingers II and III with preaxial fringe extending towards the base of fingers in males and females; (8) toe tips slightly expanded on Toes III, IV and V; (9) inner metatarsal tubercle small, ovoid and conspicuous, outer metatarsal tubercle indistinct; (10) dorsal color pattern medium brown with abundant small spots (orange in life, cream in preservative) forming a mottled pattern, a continuous stripe extends from the snout along the canthus rostralis and upper eyelid to midway between eye and axilla; (11) venter pearl white with sparse melanophores, throat color similar to dorsum in males and females; (12) conspicuous depres-

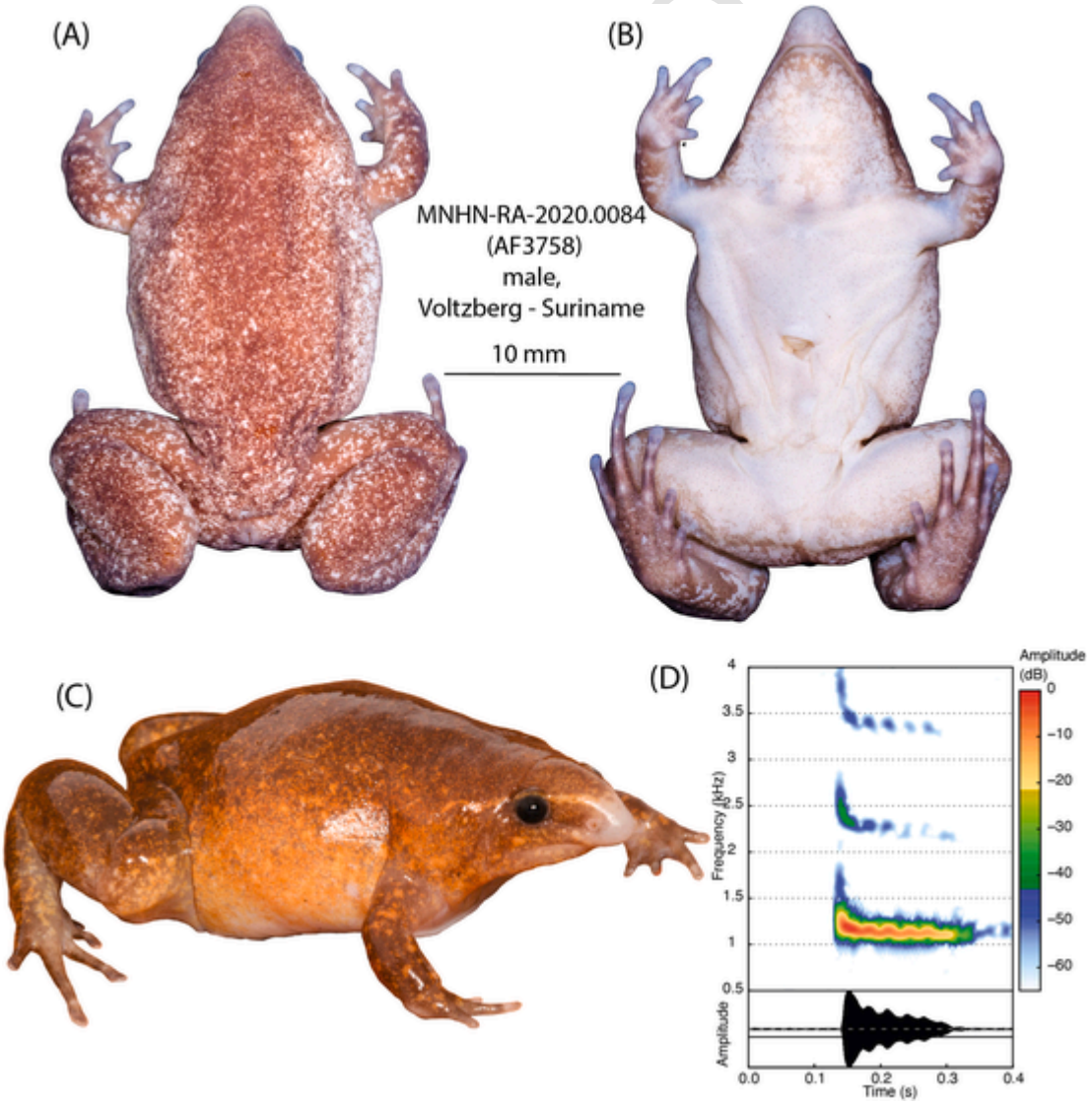

Fig. 1. Preserved adult male of *Synapturanus mirandaribeiroi* from Voltzberg, Suriname (MNHN-RA-2020.0084; field number AF3758), in dorsal view (A), in ventral view (B), same specimen in life (C) and audio spectrogram and oscillogram from a call recorded at the same locality (D). Photos by AF.

sions on the prootic and frontoparietal, sphenoid-nasal bridge and septum highly ossified, phalanges I–II of Finger III shorter than metacarpal, tibiale and fibulare only fused on extremities, axis processes with enlarged terminal parts and atlas with a bulbous neural spine; (13) call consisting in a pulsed (5–8 fused pulses) note 0.130–0.194 s in length with a downward frequency modulation (delta 22–234 Hz) and a dominant frequency at 1.10–1.47 kHz (n = 9) (Table 2).

3.1.1.6. Advertisement call Nine specimens calling from underground galleries were recorded from a distance of about 2 m at air temperatures ranging from 22 to 24 °C (temperatures in the burrows unknown). Descriptive statistics of call parameters are presented in Table 2. *S. mirandaribeiroi* emits single pulsed (5–8 fused pulses) notes (note length mean = 0.166, range 0.130–0.194 s) every 6.56 s on average (range 4.10–11.60 s). The spectral structure of the note has a developed harmonic structure and the dominant frequency is 1.25 kHz on average (range 1.10–1.47 kHz) with a strong downward modulation (ca. 0.02–0.23 kHz) (Fig. 1 and Table 2).

3.1.1.7. Remarks The call recordings from Suriname (Voltzberg) and the Manaus region (Brazil) are distinct despite the fact that these populations are closely related according to the genetic data (Fouquet et al., 2021). The pulses are more pronounced, notes are longer, the downward modulation is more marked and the dominant frequency is lower in the Suriname population compared to the Brazilian populations. Therefore, we suspect that these populations may not be conspecific, contradicting molecular data and suggesting that an in-depth investigation is warranted. This observation adds to the ambiguity surrounding the conspecificity with *S.* sp. "Taboca" and the absence of molecular and call data from the type locality of *S. mirandaribeiroi*. Nevertheless, all these populations are closely related and remain indistinguishable morphologically (external and internal) thus allowing diagnosis and comparison with other species.We doubt that the two specimens reported by Pyburn (1975) as co-occurring in Vaupés with *S. salseri* belong to *S. mirandaribeiroi*. These specimens (UTA-A-3987, UTA-A-4009) have SVL = 37.0 and 35.0 mm, respectively, are much larger than males of *S. mirandaribeiroi* (26.2–30.8 mm). Moreover, the specimens reported by Nelson & Lescure (1975) from Taracuá, Brazil, on Rio Vaupés (Melin, 1941), a locality only 20 km east of Timbo may be conspecific. Similarly, some of the specimens reported by Nelson & Lescure (1975) as *S. mirandaribeiroi*, fortunately not included in the type series, in fact belong to *S.* sp. "Eastern Guianas" (Alikéné), *S.* sp. "Manaus" (Oriximiná; Itapiranga) and *S.* sp. "Guyana" (Demerara Falls and Kartabo according to Nelson & Lescure, 1975), that are described as new hereafter.

3.1.1.8. Habitat and natural history In French Guiana and Suriname, the species was found in pristine mature *terra firme* forests, and notably often in sandy soils near inselbergs. Vocalizations are more common during and immediately after rain showers and were heard between November and December, i.e., during the beginning of the rainy season (Menin et al., 2008). Menin et al. (2007) provided detailed information about the reproduction and embryonic/larval development of this species from a population nearby Manaus, Amazonas, Brazil. Two clutches contained six and nine eggs in burrows about 5–10 cm deep below the soil surface; tadpoles hatched at stage 42 of Gosner (1960) (Menin et al., 2007). Nelson & Lescure (1975) reported ants in the stomachs of one allotype and one specimen from New River (Guyana).

3.1.1.9. Distribution and conservation status *S. mirandaribeiroi* is known from 16 populations (Fig. 2), assuming conspecificity of the related populations mentioned above and additional records from Brazil (Parque Estadual Rio Negro); Guyana (Onoro; Shudikarwau – Nelson & Lescure, 1975); and Suriname (Fredberg – Dick Lock, pers. com., Oelemarie River; Lucie River – Ouboter & Jairam, 2012; Sipaliwini – Nelson, 1973; Palumeu – Nelson & Lescure, 1975). Nelson & Lescure (1975) provided an additional locality (Tung District at 610 m elevation in Guyana) that we could not locate. This range encompasses a large portion of the Eastern Guiana Shield and includes several protected areas. The species probably occurs in the northern part of the states of Amapá, Pará, and Roraima, in Brazil. *S. mirandaribeiroi* is found between 100 and 400 m above sea level (asl).Although the number of known populations remains limited, we suggest the status of this species to be considered as Least Concern according to IUCN criteria (IUCN, 2020a). The distribution of *S. mirandaribeiroi* strikingly mirrors the one of *Anomaloglossus stepheni* (Vacher et al., 2017).

Table 2
Acoustic variables.

S. rabus (n = 1)		NL (s)	DoF (Hz)	Pulses	DeF (Hz)	internote
	NA	0.039	1642	1	169	11.20
S. salseri (n = 6)	Mean	0.079	1411	1	49	5.31
	min	0.071	1312	1	14	2.36
	max	0.090	1574	1	91	9.16
S. mirandaribeiroi (n = 9)	Mean	0.167	1251	7	148	6.57
	min	0.130	1100	5	22	4.10
	max	0.194	1471	8	256	11.56
S. zombie sp. nov. (n = 4)	Mean	0.154	1107	1	142	8.48
	min	0.147	1059	1	104	6.90
	max	0.167	1190	1	194	9.90
S. mesomorphus sp. nov. (n = 2)	Mean	0.167	1093	1	28	10.30
	min	0.160	1058	1	15	9.66
	max	0.173	1127	1	40	10.93
S. ajuricaba sp. nov. (n = 5)	Mean	0.322	1064	14	57	6.91
	min	0.282	1013	12	11	5.20
	max	0.366	1121	16	87	9.04
S. sp. "Timbo" (n = 1)	NA	0.107	1017	1	21	5.22

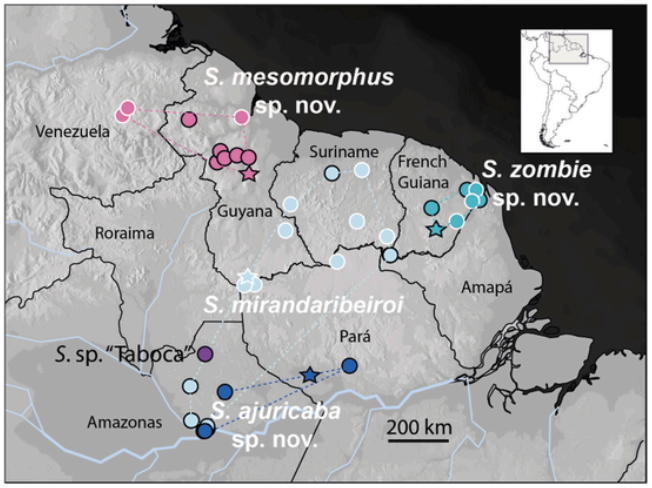

Fig. 2. Distribution of *Synapturanus* in the Eastern Guiana Shield. Symbols outlined in black indicate localities for which molecular data are available, symbols outlined in white indicate additional records from the literature [*Synapturanus mirandaribeiroi*: Nelson & Lescure (1975), Ouboter & Jairam (2012); *S. mesomorphus* sp. nov.: Nelson & Lescure (1975), Barrio-Amorós et al. (2011); *S. zombie* sp. nov.: Nelson & Lescure (1975); Dewynter et al. (2019)] for which no molecular data are available and no specimen was examined by us. Stars indicate type-localities.

3.1.1.10. Synapturanus salseri Pyburn, 1975

3.1.1.10.1. Holotype UTA-A-4011, an adult male collected by John K. Salser Jr. and William F. Pyburn the 17th of June 1973 at Timbo, Vaupés, Colombia.

3.1.1.11. Paratypes A series of 13 males and 6 juveniles collected with the holotype by Salser and Pyburn between the 17th and the 29th of June 1973 and on the 16th of March 1974; deposited as follows: UTA-A-4010, UTA-A-4021–4026, UTA-A-4036 (cleared, stained), UTA-A-4031 (series of 4 juveniles); USNM197435–7; AMNH89813; UMMZ134290; CM58829; UT46434.

3.1.1.12. Material examined Images of the male holotype UTA-A-4011, paratypes UTA-A-4010, UTA-A-4025–4026 (photos by Gregory Pandelis), AMNH89813 and USNM197435 (Fig. 3) as well as images of the following three non-type referred specimens: females ANDES-A4380, 4381; male ANDES-A4382 (Appendix B).

3.1.1.13. Definition and diagnosis (1) Medium-sized *Synapturanus* (average male SVL 25.1 [23.7–26.4 mm, n = 12]) (Pyburn, 1975); (2) head flat in lateral view; (3) eyes small, slightly smaller than eye-naris distance; (4) fingertips slightly tapering; (5) subarticular tubercles barely distinct on Finger III, not visible on the other fingers; (6) metacarpal tubercle large and prominent; (7) Fingers II and III with a rudimentary preaxial fringe extending towards the base of fingers in males and females; (8) toe tips slightly expanded on Toes III, IV and V; (9) inner metatarsal tubercle small but conspicuous, outer metatarsal tubercle indistinct; (10) dorsal color pattern medium brown with sparse spots (orange to gray in life, cream in preservative), a discontinuous stripe extends from the snout along the canthus rostralis and upper eyelid to midway between eye and axilla; (11) venter pearl white with sparse melanophores, throat gray in males and females; (12) inconspicuous depressions on the prootic and frontoparietal, sphenoid-nasal bridge and septum highly ossified, phalanges I–II of Finger III equal to metacarpal in length, tibiale and fibulare only fused on extremities, axis processes without enlarged terminals parts and atlas without a bulbous neural spine; (13) call consisting in a tonal note 0.07–0.09 s in length with a slight downward frequency modulation (delta 14–91 Hz) and a dominant frequency at 1.31–1.57 kHz (n = 6) (Table 2).

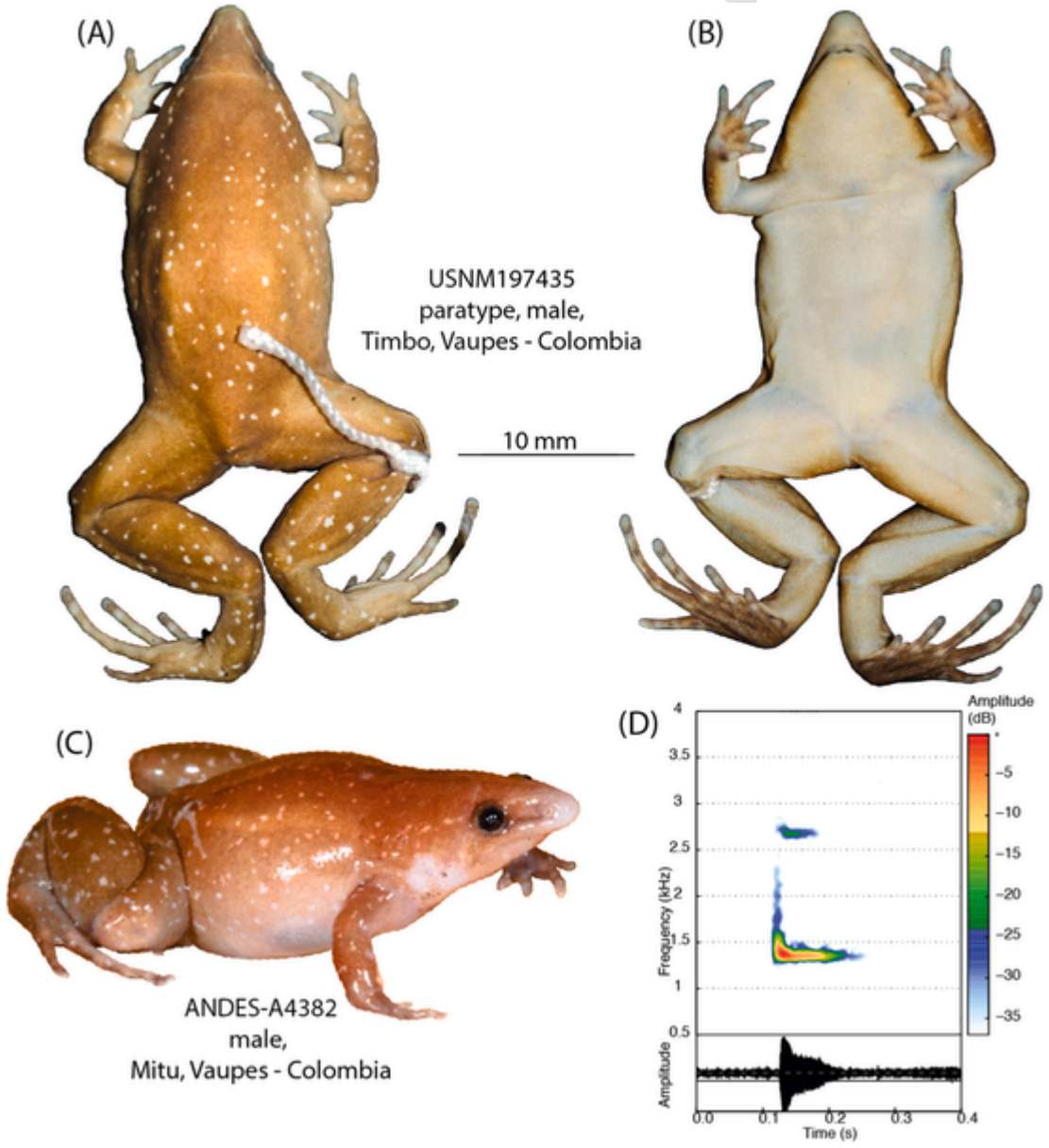

Fig. 3. Preserved paratype USNM 197435 (Photos by P.P.) of *Synapturanus salseri* in dorsal (A) and ventral (B) views; photo in life of ANDES-A 4382 (AF4186) a male specimen from Mitu (C) (photo by AF), Vaupés Colombia; and audio spectrogram and oscillogram from the same locality (D).

3.1.1.14. Advertisement call Six males calling from underground galleries were recorded from a distance of about 2 m at air temperatures ranging from 22 to 24 °C (temperatures in the burrows unknown). Descriptive statistics of call parameters are presented in Table 2. *S. salseri* emits single tonal notes (note length mean = 0.078, range 0.071–0.090 s) every 5.31 s on average (range 2.36–9.16 s). The spectral structure of the note has a developed harmonic structure and the dominant frequency is 1.41 kHz on average (range 1.31–1.57 kHz) with a slight downward modulation (ca. 0.01–0.09 kHz) (Fig. 3, Table 2).

3.1.1.15. Remarks A call recorded by Pyburn from Timbo, Vaupés, Colombia, was probably assigned in error to *S. salseri* by Fouquet et al., 2021 since the dominant frequency of this call (1.02 kHz) does not match the values provided by Pyburn (1975) in the original description (1.4 kHz). Based on the lower frequency, this call recording may in fact correspond to the call of the larger species, identified as *S. mirandaribeiroi* by Pyburn (1975), a species co-occurring with *S. salseri*, and possibly yet unnamed as this call does not match that of *S. mirandaribeiroi* either. Additional recordings from Mitu, Vaupés, Colombia (10 km from Timbo), match the sonogram (dominant frequency of 1.4 kHz) provided by Pyburn (1975) and were used in the description of the advertisement call above. A recorded calling specimen from Mitu (ANDES-A4382) is morphologically similar to the type specimens and Pyburn's description (Fig. 3).

3.1.1.16. Habitat and natural history This species occurs in pristine and secondary growth *terra firme* forest. Pyburn (1975) described a clutch of four eggs and two other nests with six larvae and four froglets, respectively. They were all found in underground chambers guarded by a male connected to the surface by smooth walled burrows up to 15 cm deep directly below the root layer. Larvae are endotrophic after hatching, which happens at least at stage 37 of Gosner (1960). Pyburn (1975) also reported on the stomachs of four frogs that contained 33 ants of the genera *Solenopsis* and *Pheidole*, and one spider.

3.1.1.17. Distribution and conservation status The species is only known with certainty from Timbo, Vaupés, Colombia, and surrounding areas (Mitu). *S. salseri* occurs at about 200 m asl.Given that the range of the species likely extends further, we suggest this species to be considered as Data Deficient according to IUCN criteria (IUCN, 2020a,b).

3.1.1.18. Synapturanus zombie sp. nov. *S. mirandaribeiroi* Nelson & Lescure, 1975.*Synapturanus* sp. "Eastern Guianas" Vacher et al., 2020; Fouquet et al., 2021.

3.1.1.19. Holotype MNHN-RA-2020.0091 (field number AF3986), an adult male collected by E. Courtois and M. Dewynter on the 14th of November 2018 at Itoupé, French Guiana (3.0230°N 53.0955°W, ~600 m elevation; Fig. 4).

3.1.1.20. Paratypes Five males: MNHN-RA-2020.0090 (AF3985), collected with the holotype, MNHN-RA-2020.0088 (AF3722), MNHN-RA-2020.0089 (AF3723), collected by A Fouquet, E. Courtois, B. Villette and M. Dewynter on the 16th of January 2016 at Itoupé, French Guiana (3.0230°N 53.0955°W), MNHN-RA-1982.131 collected by L. Gruner on the 11th of November 1969 at Alikéné, French Guiana (3.2090°S 52.4020°W); MNHN-RA-2020.0086 (AF1315) collected by S. Barrioz on the 6th of November 2013 at Manare, French Guiana (4.1833°N 52.1500°W); and three females: MZUSP159220 (MTR24135) collected by S. Marques de Souza, J. Dias Lima and A. Fouquet on the 2nd of December 2012 at Oiapoque, Amapá, Brazil (3.8794°N 51.7710°W); MNHN-RA-2020.0085 (AF0525) collected by M. Dewynter on the 19th of April 2008 at Saul, French Guiana (3.6376°N 53.2137°W); MNHN-RA-2020.0087 (AF3573) collected by A. Fouquet, E. Courtois, B. Villette and M. Dewynter on the 16th of January 2016 at Itoupé, French Guiana (3.0230°N 53.0955°W).

3.1.1.21. Definition and diagnosis (1) Large-sized *Synapturanus* (average male SVL 39.3 mm [37.0–40.6, n = 4], female SVL 39.9 mm [38.7–42.1, n = 3]) (Table 1); (2) head dorsally convex in lateral view; (3) eyes small, slightly larger than half the size of the eye-naris distance; (4) fingertips tapering except on Finger IV that has a rounded tip; (5) subarticular tubercles not visible on fingers; (6) thenar tubercle large and prominent, palmar tubercle indistinct; (7) fingers with pre- and postaxial fringes (except postaxially on Finger IV), particularly developed on Fingers II and III where fringes extend towards the base of fingers in males and females; (8) toe tips expanded; (9) inner metatarsal tubercle ovoid and conspicuous, outer metatarsal tubercle indistinct; (10) dorsal color pattern medium brown with abundant spots and blotches over the back, head, arms and legs (orange in life, cream in preservative), absence of stripe along the canthus rostralis and upper eyelid; (11) venter pearl white with sparse tiny melanophores, throat similarly colored as dorsum in males and females; (12) conspicuous depressions on the prootic and frontoparietal, sphenoid-nasal bridge and septum highly ossified, axis processes with enlarged terminals parts and atlas with a bulbous neural spine, phalanges I–II of Finger III shorter than metacarpal, tibiale and fibulare only fused on extremities; (13) call consisting of a tonal note 0.147–0.167 s in length with a downward frequency modulation (delta 104–194 Hz) with a dominant frequency at 1.06–1.19 kHz (n = 4) (Table 2).*S. zombie* sp. nov. can be distinguished from *S. rabus* in being much larger (SVL = 37.0–42.1 mm in *S. zombie* sp. nov. vs. 16.2–19.0 mm in *S. rabus*); in having smaller eyes (3.9% of SVL in *S. zombie,* 7.3% in *S. rabus*); fringes on Fingers II and III (absent in *S. rabus*); a convex head in lateral view (flat in *S. rabus*); a medium brown dorsum with numerous orange spots and blotches in life (vs. unspotted and uniformly dark brown in *S. rabus*); in lacking a stripe along the canthus rostralis and upper eyelid (vs. stripe present in *S. rabus*); in emitting a call consisting of longer notes (0.147–0.167 s in *S. zombie* vs. 0.039 s in *S. rabus*); and in having unfused tibiale and fibulare (vs. fused in *S. rabus*).*S. zombie* sp. nov. can be distinguished from *S. salseri* in being larger (SVL = 37.0–40.6 mm in males of *S. zombie* sp. nov. vs. 23.7–26.4 mm in males of *S. salseri*); in having smaller eyes (3.9% of SVL in *S. zombie* sp. nov. vs. 5.4% in *S. salseri*); extensive fringes on Fingers II and III (vs. rudimentary fringes in *S. salseri*); a convex head in lateral view (vs. flat in *S. salseri*); a medium brown dorsum with numerous orange spots and blotches in life (vs. sparse spots in *S. salseri*); in lacking a stripe along the canthus rostralis and upper eyelid (vs. presence of a discontinuous stripe in *S. salseri*); in emitting a call consisting of longer notes (0.147–0.167 s in *S. zombie* vs. 0.079 s in *S. salseri*); and in having conspicuous depressions on the prootic and frontoparietal (vs. inconspicuous in *S. salseri*), axis processes with enlarged terminals parts (vs. not enlarged in *S. salseri*) and atlas with a bulbous neural spine (vs. not bulbous in *S. salseri*), phalanges I–II of Finger III shorter than metacarpal (vs. longer in *S. salseri*).*S. zombie* sp. nov. can be distinguished from *S. mirandaribeiroi* in being larger (SVL = 37.0–40.6 mm in males of *S. zombie* vs. 26.6–30.8 mm in males of *S. mirandaribeiroi*); in having smaller eyes (3.9% of SVL in *S. zombie* sp. nov. vs. 5.2% in *S. mirandaribeiroi*); Fingers II and III tapering with well-developed fringes (vs. rudimentary fringes present and tip of these fingers rounded in *S. mirandaribeiroi*); a medium brown dorsum with numerous orange spots and blotches in life (vs. medium brown dorsum with diffuse mottled pattern in *S. mirandaribeiroi*); in lacking a stripe along the canthus rostralis and upper eyelid (vs. stripe present in *S. mirandaribeiroi*); and in emitting a call consisting of tonal notes (vs. pulsed in *S. mirandaribeiroi*).

3.1.1.22. Description of the holotype An adult male, 37.0 mm SVL; body stout; head as long as wide, HL 20% of SVL; dorsal and ventral skin smooth from head to cloaca; linea masculina visible through the translucent ventral skin in life, extending ventrolaterally from axilla to groin; supratympanic fold running from the posterior corner of the eye, curving towards the axilla, continuous with an occipital (postcephalic) fold and a gular fold; presence of a thoracic fold; snout long and strongly protruding, projecting well beyond the end of the lower jaw (2.73 mm), tip rounded in dorsal and lateral view. Eyes small, 66% of EN; nares located laterally, closer to the tip of the snout (1.75 mm)

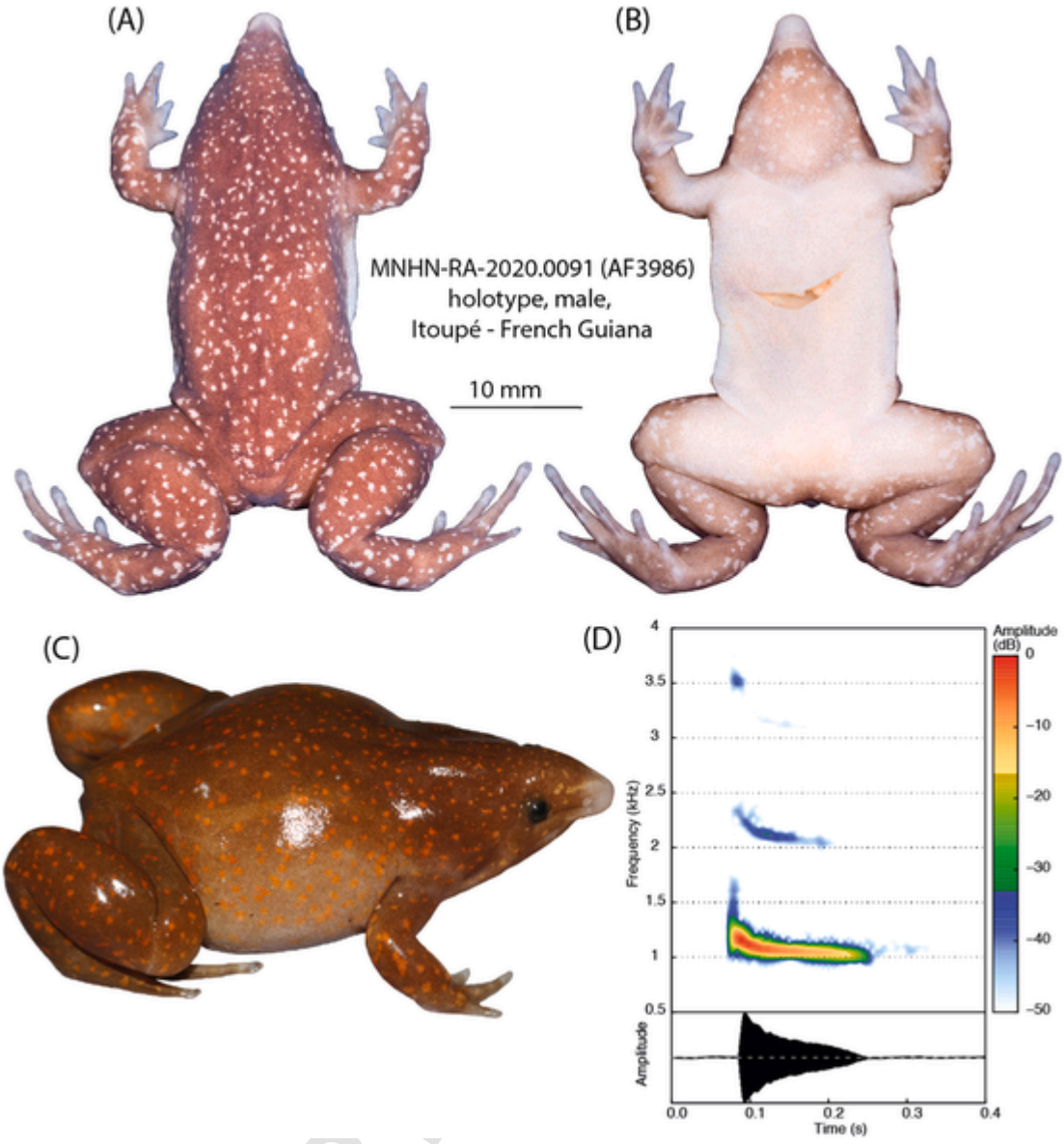

Fig. 4. Preserved holotype MNHN-RA-2020.0091 of *Synapturanus zombie* sp. nov. in dorsal (A) and ventral (B) views, photo of holotype in life (C); and audio spectrogram and oscillogram of a call of an unvouchered individual recorded from the type locality (D). Photo in life by M.D.

than to the eye (2.27 mm); canthus rostralis rounded, loreal region strongly concave, grooved; IN 34% of HW; EN 32% of HL. Tympanum concealed and only distinct anteroventrally, obscured posterodorsally by the supratympanic fold; choanae small (50% of ED), drop shaped, located anterolaterally, no odontophore.Forelimb robust, skin smooth; HAND 20% of SVL; Finger II longer than Finger I when fingers adpressed; fingers short, tips tapering, unwebbed, with pre- and postaxial fringes (except postaxially on Finger IV), particularly developed on Fingers II and III where fringes extend towards the base of fingers; no finger discs; relative length of adpressed fingers III > IV > II > I; subarticular tubercles not visible on fingers; thenar tubercle large and prominent, palmar tubercle indistinct. Glandular unpigmented supracarpal pad.Hind limb robust, skin smooth; TL 35% of SVL; FL 37% of SVL; relative length of adpressed toes IV > III > V > II > I; Toe I very short, its tip reaching the base of Toe II when toes adpressed; toes without discs, tips as large as width of toes. Toes unwebbed with narrow pre- and postaxial fringes. Subarticular tubercles not visible on toes; inner metatarsal tubercle ovoid, large (1.2 mm) and prominent, outer metatarsal tubercle indistinct. Metatarsal fold absent.

3.1.1.23. Color of holotype in life Dorsal color medium brown with numerous orange spots and blotches over the back, head, arms and legs. Flanks light brown with abundant orange spots and blotches. Absence of a stripe along the canthus rostralis and upper eyelid, but a few aligned spots form a discontinuous series. Snout white, unpigmented. Throat medium brown with orange spots; belly translucent pearl white with small melanophores (Fig. 4). Upper and lower arm and dorsal surfaces of thigh, shank and tarsus similar to the dorsum in color. Glandular supracarpal pad translucent white.

3.1.1.24. Color of holotype in preservative After four years in 70% ethanol, colors of the specimen faded with the orange spots and blotches turning white as well as the glandular supracarpal pad (Fig. 4).

3.1.1.25. Variation For morphometric variation see Table 1. Sexual dimorphism consists of the presence of a supracarpal pad in males, and differences in body size, although males and females overlap in SVL and this sexual dimorphism remains subtle. Linea masculina visible in life through the translucent ventral skin in males. Yellow ovaries are visible in life through the translucent skin in females, and in preserva-

tive in females. Coloration varies little across specimens examined (Fig. 5), ground dorsal coloration varies from light to medium brown with orange or yellowish spots in life.

3.1.1.26. Advertisement call Four specimens calling from underground galleries were recorded from a distance of about 2 m at air temperatures ranging from 22 to 24 °C (temperatures unknown inside the galleries). Descriptive statistics of call parameters are presented in Table 2. *S. zombie* sp. nov. emits single tonal notes (note length mean = 0.154, range 0.147–0.167 s) every 8.47 s on average (range 8.20–9.90 s). The spectral structure of the note has a developed harmonic structure and the dominant frequency is 1.11 kHz on average (range 1.06–1.19 kHz) with a strong downward modulation (ca. 0.1–0.2 kHz) (Fig. 4, Table 2).

3.1.1.27. Habitat and natural history *S. zombie* sp. nov. has been found in well-drained *terra firme* soils, in primary forest on the slopes of massifs and sandy soils near inselbergs. They dig galleries from which the males call, spaced a few meters apart from each other, during and after heavy rain showers during the weeks preceding the rainy season (October–November). Females probably use the same galleries since they have been found while searching for the provenance of a call. We assume that the mode of reproduction of this species is similar to that of the related species for which it is documented, although this needs to be confirmed by field observations.

3.1.1.28. Etymology The specific epithet is a noun in apposition referring to zombies, fictional undead corporeal revenants, originating from Haitian folklore and omnipresent in pop culture movies. The call of this species is only heard during and after heavy rain showers, when herpetologists are often not properly equipped, thus ending up soaked and digging with their bare hands in the mud in the midst of thunderstorms, reminiscent of zombies extracting themselves from the ground.

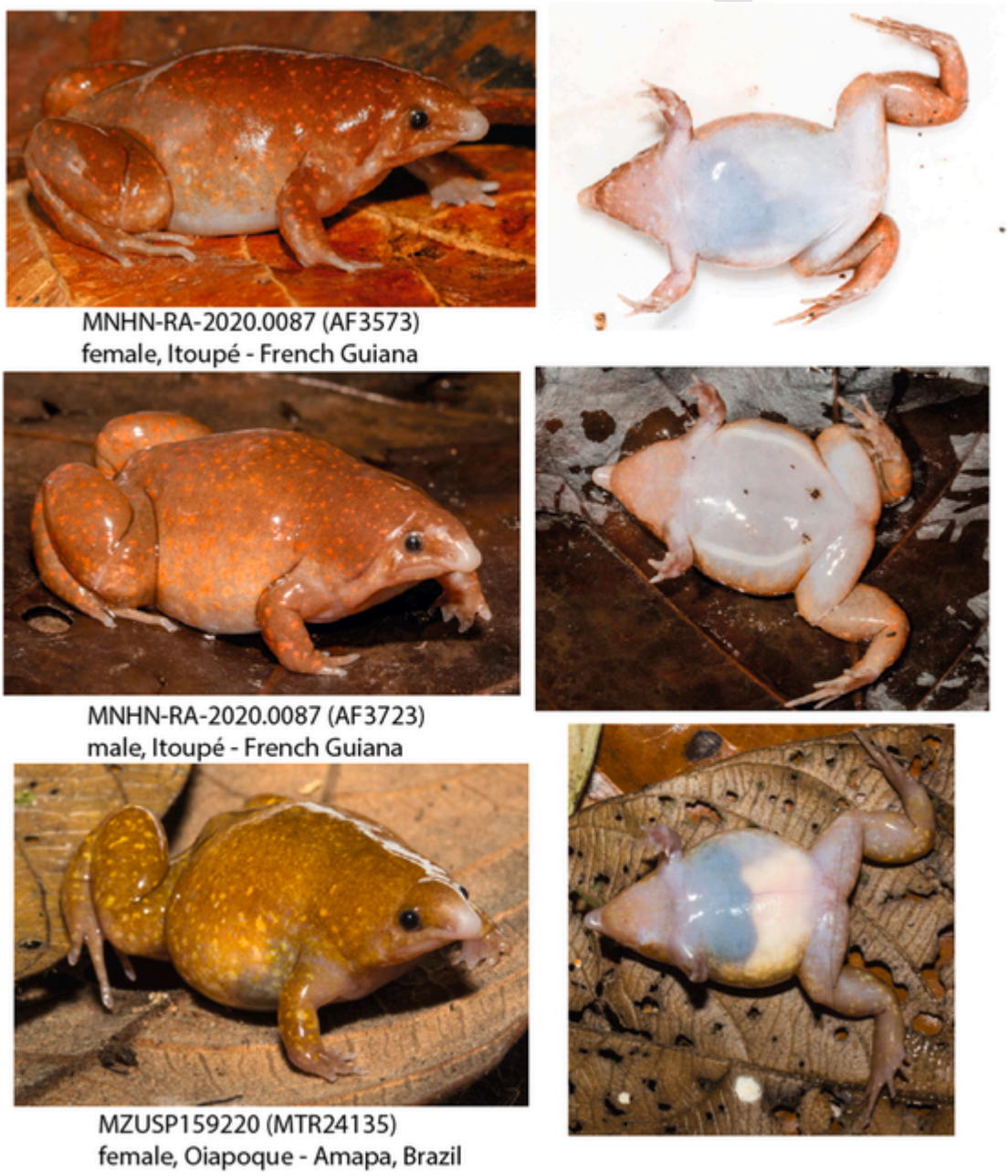

Fig. 5. Variation among specimens of *Synapturanus zombie* sp. nov. in life. Photos by A.F.

3.1.1.29. Distribution and conservation status *S. zombie* sp. nov. is only known from six groups of populations in French Guiana (Savane Virginie/Mataroni, Trois Pitons, Saut Maripa, Alikéné, Saul, Itoupé, Mont Chauve) and one population in Amapá, Brazil (Oiapoque) (Fig. 2). An additional likely locality in Amapá is "Rivière Lunier" (Upper Rio Calçoene = Haut-Carsevenne) (2.3734°N, 51.3782°W) but it corresponds to a lost specimen from MNHN (J. Lescure, pers. comm.). This species is most likely endemic to the easternmost part of the Guiana Shield. In French Guiana, *S. mirandaribeiroi* is found in the southwestern corner of the territory and the species do not seem to co-occur, suggesting a boundary in their respective distributions and possibly exclusion. *S. zombie* sp. nov. is absent from the northwestern part of French Guiana with a putative limit at the level of the Approuague basin, a distribution pattern similar to that of several other species such as *Amazophrynella teko* Rojas-Zamora, Fouquet, Ron, Hernández-Ruz, Melo-Sampaio, Chaparro, Vogt, Carvalho, Pinheiro, Ávila, Farias, Gordo, and Hrbek, 2018; *Leptodactylus longirostris* (Boulenger, 1882) or *Pristimantis* sp. (= *P.* sp. 1 of Fouquet et al., 2013). *S. zombie* sp. nov. is found between 100 and 600 m asl. Its range is most likely small and the populations seem isolated from each other, but it is such a difficult species to detect that this remains speculative.Given the uncertainties regarding its distribution and population status, we suggest considering the species as Data Deficient according to IUCN criteria (IUCN, 2020a,b). Some of the known populations occur in protected areas in French Guiana (i.e., in the Parc Amazonien de Guyane).

3.1.1.30. Synapturanus mesomorphus sp. nov. *S. mirandaribeiroi* Nelson & Lescure, 1975; Ernst et al., 2005.*S. salseri* Kok & Kalamandeen, 2008; Cole et al., 2013.*Synapturanus* sp. "Guyana" Vacher et al., 2020; Fouquet et al., 2021.

3.1.1.31. Holotype MTD48012 (field number RE-040), an adult female, collected by Monique Hölting and Raffael Ernst the 21st of May 2010 at Iwokrama, Guyana (4.6713°N, 58.7751°W, ~160 m elevation; Figs. 6 and 7).

3.1.1.32. Paratypes Six males: AMNH166450 (JC7727), collected by C.J. Cole and C.R. Townsend between the 3rd and 6th of March 1998 in Magdalen's Creek camp, near (275 m).NW bank of the Konawaruk River, Guyana (5.2186°N 59.0453°W); SMNS12077–78 (MABM0202, MABM0102) collected by R. Ernst on the 16th and the 14th of November 2002, respectively, in Mabura Hill Forest Reserve, Guyana (5.1553°N 58.6997°W); RBINS4202 (PK1397), collected by P.J.R. Kok, P. Benjamin and G. Seegobin on the 28th of March 2006 in Kaieteur National Park, Guyana (5.1333°N 59.4167° W); RBINS4204 (PK1577), collected by P.J.R. Kok, P. Benjamin and G. Seegobin on the 26th of June 2006 in Kaieteur National Park, Guyana (5.1333°N 59.4000° W); USNM588794 (BPN3813), collected by A. Snyder on the 5th of March 2014 at Bay Camp, Potaro-Siparuni, Guyana (5.0115°N 59.6431°W). Seven females: USNM566235 (JC7845), by C.J. Cole and C.R. Townsend between the 10 and 11th of March 1998 in Magdalen's Creek camp, near (275 m) NW bank of the Konawaruk River, Guyana (5.2186°N 59.0453°W); RBINS4201 (PK1396), collected by P.J.R. Kok, P. Benjamin and G. Seegobin on the 28th of March 2006 in Kaieteur National Park, Guyana (5.1333°N 59.4167°W); RBINS4205 (PK1641), collected by G. Seegobin in November 2006 in Kaieteur National Park, Guyana (5.1333°N 59.4167°W); RBINS4206–07 (PK1137, PK1143), col-

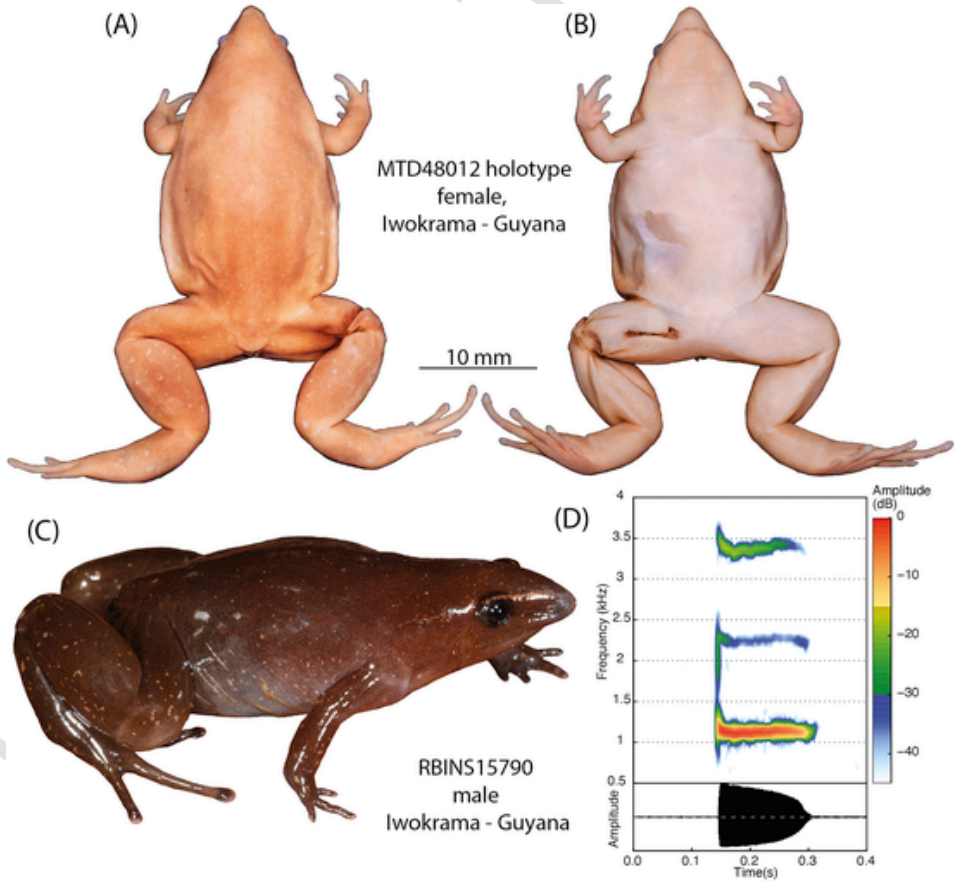

Fig. 6. Preserved holotype MTD48012 of *Synapturanus mesomorphus* sp. nov. in dorsal (A) and ventral (B) views; photo in life of RBINS15790 (PK3513) (C); sonogram of a call record from the type locality (D) (photo in life by P.J.R.K.).

Fig. 7. Variation among specimens of *Synapturanus mesomorphus* sp. nov. in life (photos by M.H. - holotype and P.J.R.K. – RBINS4204 & RBINS15789).

lected by F. Marco in January 2006 in Kaieteur National Park, Guyana (5.1969°N 59.4817°W); USNM588793 (BPN3762), collected by A. Snyder on the 11th of March 2014 at Bay Camp, Potaro-Siparuni, Guyana (5.0115°N 59.6431°W); MTD49061 (RE-MH27), collected by M. Hölting and R. Ernst on the 23rd of June 2014 in Iwokrama Forest Reserve, Guyana (4.4942°N, 58.7759°W). One juvenile: RBINS4203 (PK1570), collected by P.J.R. Kok, P. Benjamin and G. Seegobin on the 23rd of June 2006 in Kaieteur National Park, Guyana (5.1333°N 59.4167° W).

3.1.1.33. Material examined We additionally examined 10 referred specimens (see Appendix B).

3.1.1.34. Definition and diagnosis (1) Medium-sized *Synapturanus* (average male SVL 24.7 mm [22.9–26.0, $n = 6$], female SVL 27.9 mm [26.3–29.4, $n = 11$]) (Table 1); (2) head convex in lateral view; (3) eyes small, slightly smaller than eye-naris distance; (4) fingertips rounded; (5) subarticular tubercles not visible on fingers; (6) thenar tubercle barely distinct, palmar tubercle indistinct; (7) Fingers II and III with preaxial fringes in males and females, extending towards the base of fingers; (8) toe tips expanded; (9) inner metatarsal tubercle small, ovoid, outer metatarsal tubercle indistinct; (10) dorsal color pattern dark to light brown with sparse small speckles and blotches over the back, head, arms and legs (beige in life, cream in preservative), a more or less continuous stripe (often broken in small flecks/spots) extends

from the snout along the canthus rostralis and upper eyelid to midway between eye and axilla; (11) venter pearl white with melanophores, throat color similar to dorsal color in males and females; (12) inconspicuous depressions on the prootic and frontoparietal, sphenoid-nasal bridge and septum highly ossified, axis processes with enlarged terminals parts and atlas large with an inconspicuous bulbous neural spine, phalanges I–II of Finger III equal to metacarpa in length, tibiale and fibulare only fused on extremities; (13) call consisting in a tonal note 0.160–0.173 s in length with a dominant frequency at 1.06–1.13 kHz (n = 2) (Fig. 6, Table 2).*S. mesomorphus* sp. nov. can be distinguished from *S. rabus* in being larger (SVL = 22.9–29.4 mm in *S. mesomorphus* sp. nov. vs. 16.2–19.0 mm in *S. rabus*); in having smaller eyes (5.1% of SVL in *S. mesomorphus* sp. nov. vs. 7.3% in *S. rabus*); preaxial fringes on Fingers II and III (vs. no fringes in *S. rabus*); a convex head in lateral view (vs. flat in *S. rabus*); a brown dorsum with sparse speckles and beige blotches in life (vs. dorsum uniformly brown in *S. rabus*); a call consisting of longer notes (0.160–0.173 s in *S. mesomorphus* sp. nov. vs. 0.039 in *S. rabus*); and tibiale and fibulare only fused on extremities (vs. entirely fused in *S. rabus*).*S. mesomorphus* sp. nov. is most similar to *S. salseri*, from which it can be distinguished by having a convex head in lateral view (flat in *S. salseri*); a call consisting of longer notes (0.160–0.173 s in *S. mesomorphus* sp. nov. vs. 0.079 in *S. salseri*); and axis processes with enlarged terminal parts (vs. not enlarged in *S. salseri*) and atlas with a bulbous neural spine (vs. not bulbous in *S. salseri*).*S. mesomorphus* sp. nov. can be distinguished from *S. mirandaribeiroi* in having a smaller body size (SVL = 22.9–26.0 mm in males of *S. mesomorphus* vs. 26.6–30.8 mm in males of *S. mirandaribeiroi*); a brown dorsal coloration with sparse speckles and blotches (diffuse mottled pattern in *S. mirandaribeiroi*); a call consisting of tonal notes (vs. pulsed in *S. mirandaribeiroi*); and inconspicuous depressions on the prootic and frontoparietal (vs. conspicuous in *S. mirandaribeiroi*), phalanges I–II of Finger III equal to metacarpa in length (vs. shorter in *S. mirandaribeiroi*).*S. mesomorphus* sp. nov. can be distinguished from *S. zombie* sp. nov. in being smaller (SVL = 22.9–26.0 mm in males of *S. mesomorphus* vs. 37.0–40.6 mm in males of *S. zombie* sp. nov.); in having a light to dark brown dorsal coloration with sparse beige speckles and blotches (vs. medium brown with numerous orange spots and blotches in *S. zombie*); a stripe running along the canthus rostralis and the upper eyelid to midway between eye and axilla (vs. stripe absent in *S. zombie* sp. nov.); a call lacking downward frequency modulation (vs. 104–194 Hz decrease in *S. zombie* sp. nov.); and inconspicuous depressions on the prootic and frontoparietal (vs. conspicuous in *S. zombie* sp. nov.), phalanges I–II of Finger III equal to metacarpals in length (vs. shorter in *S. zombie* sp. nov.).

3.1.1.35. Description of the holotype (Fig. 6) An adult female, 29.4 mm SVL; body stout; head slightly wider than long, HL 20% of SVL; dorsal and ventral skin smooth; supratympanic fold running from the posterior corner of the eye, curving towards the axilla, continuous with an occipital (postcephalic) fold and a gular fold; presence of a thoracic fold; snout long and strongly protruding, projecting well beyond the end of the lower jaw (2.0 mm), rounded in dorsal and lateral view. Eyes small, 85% of EN; nares located laterally closer to the tip of the snout (1.03 mm) than to the eye (1.91 mm); canthus rostralis rounded, loreal region strongly concave with a groove between the naris and the eye; IN 29% of HW; EN 32% of HL. Tympanum concealed and only distinct anteroventrally, obscured posterodorsally by a supratympanic fold; choanae small (50% of ED), drop shaped, located anterolaterally, no odontophore.Forelimb robust, skin smooth; HAND 16% of SVL; Finger II longer than Finger I when fingers adpressed; fingers short with rounded tips, unwebbed, with preaxial fringes on Fingers II and III extending towards the base of fingers; no finger discs; relative lengths of adpressed fingers III > IV > II > I; subarticular tubercles not visible on fingers; thenar tubercle large and prominent, palmar tubercle indistinct.Hind limb robust, skin smooth; TL 40% of SVL; FL 38% of SVL; relative length of adpressed toes IV > III > V > II > I; Toe I very short, its tip reaching the base of Toe II when toes adpressed; toe without discs; Toes II, III, IV and V have expanded tips. Toes unwebbed; narrow preaxial fringes on Toes II–V and postaxial fringes on Toes II–IV; subarticular tubercles not visible on toes; inner metatarsal tubercle ovoid (0.85 mm); outer metatarsal tubercle indistinct; metatarsal fold absent.

3.1.1.36. Color of holotype in life Dorsal color light brown with few, very small beige speckles over the back and head, more abundant on arms and legs. Flanks light grayish brown with larger and more abundant beige blotches. More or less continuous stripe along the canthus rostralis and upper eyelid, formed by aligned speckles. Snout gray. Throat light brown, immaculate; belly translucent gray with small melanophores (Fig. 7). Upper and lower arm and dorsal surfaces of thigh, shank and tarsus similar to the flanks in color.

3.1.1.37. Color of holotype in preservative After ten years in 70% ethanol, colors of the specimen generally faded (Fig. 6).

3.1.1.38. Variation For morphometric variation see Table 1. Sexual dimorphism is apparent in size (SVL of males and females do not overlap) and in the presence of a supracarpal pad in males (poorly visible in preservative). Ovaries are visible through the translucent skin in gravid females. Background coloration varies extensively across specimens from light brown to dark brown. Spot color varies from white, beige to orange. The stripe along the canthus rostralis and upper eyelid can be markedly discontinuous (as in the holotype), or extending only a few mm posteriorly to the eye (RBINS15789) to as long as extending to the axilla (RBINS15790) (Fig. 7). This stripe can either be narrow or relatively broad, notably along the canthus rostralis (RBINS15789).

3.1.1.39. Advertisement call Two specimens calling from underground galleries were recorded from a distance of about 2 m at air temperatures ranging from 22 to 25 °C (temperatures in the galleries unknown). Descriptive statistics of call parameters are presented in Table 2. *S. mesomorphus* sp. nov. emits single tonal notes (note length mean = 0.166, range 0.160–0.173 s) every 10.29 s on average (range 9.66–10.93 s). The spectral structure of the note has a developed harmonic structure and the fundamental (dominant frequency) is 1.09 kHz on average (range 1.06–1.13 kHz) with a slight downward modulation between the beginning and the end of the note (ca. 0.01–0.04 kHz) (Fig. 6, Table 2).

3.1.1.40. Habitat and natural history The habitats where *S. mesomorphus* sp. nov. was found range from clearings in white sand forest to well-drained mixed forest on white sand and brown sand (ferralic arenosols) in the vicinity of riverine floodplain forest on alluvial soils, but always in un-inundated areas. Males call from burrows in the ground, below the leaf litter and exclusively during drizzling or heavy rainfalls. Calling activity seems triggered by the sound of the rain drops on the ground. Most of our specimens were collected in the early morning in pitfall traps, indicating active movements above the ground at night, or were actively excavated from small burrows while calling, during or shortly after rainfall. One uncatalogued specimen (PK3789) was found active on the ground at dusk. Reproduction and clutches have never been directly observed. However, we assume that eggs are laid in burrows below the soil surface and that tadpoles do not feed and complete their development within the burrow as in other related species. Nelson & Lescure (1975) reported on the stomach content of a specimen from Demerara Falls containing only ants, which is consistent with the gut contents of one dissected specimen (RBINS15789). However, the stomachs of some other specimens that were dissected (e.g., paratype RBINS4202 and RBINS15812) contained a large number of termites, including large soldiers. In Mabura Hill, no record of calling activity was made outside a very short reproductive period, which was restricted to only a very few nights annually (Ernst et al., 2005).

3.1.1.41. Etymology The specific epithet comes from the Greek *mesos* (middle, intermediate) and *morphē* (sort, appearance, form) and refers to the intermediate morphology of the species between the easternmost species of the eastern clade and the species of the western clade (Fouquet et al., 2021).

3.1.1.42. Distribution and conservation status This species is currently known from eight localities in Guyana (Mabura Hill Forest Reserve, Iwokrama Forest Reserve, Kaieteur National Park, Bay Camp, Meamu River, Kuribrong, Konawaruk Camp, Kartabo) on the eastern edge of Pantepui, or at the boundaries between Pantepui and the lowlands of the Eastern Guiana Shield (Fig. 2). *S. mesomorphus* sp. nov. might occur in neighboring Venezuela (La Escalera, Sierra de Lema 6.6670°N 62.4170°W - Barrio-Amorós et al., 2011; Cerro Santa Rosa Serrania del Supamo 6.6170°N 62.4500°W; Barrio-Amorós and Brewer-Carías, 1999) and in the southern part of Guyana where it could enter in contact with *S. mirandaribeiroi*. *S. mesomorphus* sp. nov. is found between 100 and 580 m asl. It is unlikely that this species extends much further than its small currently recognized range. The area where this species occurs is heavily impacted by past and ongoing gold-mining activities (Dezécache et al., 2017). Although some of the known populations are within protected areas (Iwokrama, Kaieteur, Mabura) a significant portion of the range of the species is threatened by illegal activities, such as the aforementioned mining and rampant deforestation (Ernst et al., 2006).Considering the small number of known populations (<10), the small range (<20,000 km^2) and their likely decline in the upcoming future we suggest that *S. mesomorphus* sp. nov. should be considered as Vulnerable (B1ab(iii)) by the IUCN.

3.1.1.43. Synapturanus ajuricaba sp. nov. *S. mirandaribeiroi* Nelson & Lescure, 1975.*S. salseri* Lima et al., 2006; Peloso et al., 2014.*Synapturanus cf.* salseri Menin et al., 2007.*Synapturanus* sp. "Manaus" Vacher et al., 2020; Fouquet et al., 2021.

3.1.1.44. Holotype INPA-H38464 (field n°CTGA-1804), an adult female, collected by A. Almeida, R.R. Rojas, A. Oliveira and O. Pereira on the 1st of December 2013 on the right bank of Trombetas River, Pará, Brazil (1.3818°S 56.8630°W, ~100 m elevation; Fig. 8).

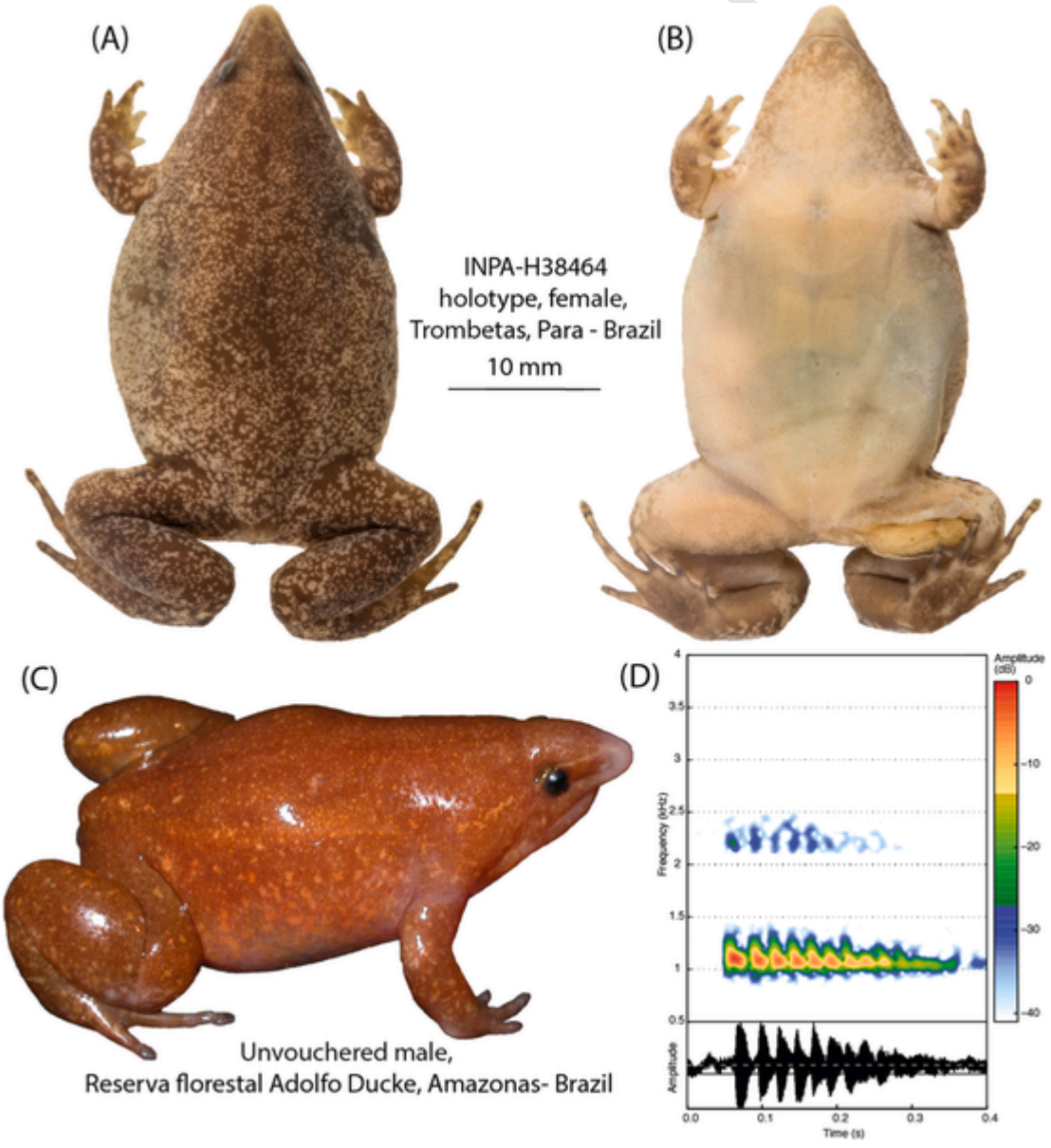

Fig. 8. Preserved holotype INPA-H 38464 of *S. ajuricaba* sp. nov. in dorsal (A) and ventral (B) views; photo in life of an unvouchered specimen (photo by W.E. Magnusson and A.P. Lima) (C); sonogram of a call record from Reserva Florestal Adolpho Ducke (D).

3.1.1.45. Paratypes Five males: MPEG29453 (CN370), MPEG29454 (CN373), MPEG29456 (CN416), MPEG29457 (CN523), MPEG29458 (CN590) collected by M.S. Hoogmoed and W. Rocha between the 16th and the 26th of April 2008 at Floresta Estadual de Trombetas, Pará, Brazil (0.9628°S 55.5223°W); and two females: INPA-H28519 collected by V.T. de Carvalho on the 1st of September 2007 at Sítio Renato Cintra, Ponte Cacau Pereira, Amazonas, Brazil (3.1050°S 60.0691°W); and INPA-H35751 collected by A.F. Palmeirim on the 13th of June 2015 at Ilha Sapupara, Amazonas state, Brazil (1.8924°S 59.4487°W).

3.1.1.46. Diagnosis and comparisons (1) Medium-sized *Synapturanus* (average male SVL 31.8 mm [29.3–33.2, $n = 5$], female SVL 36.5 mm [35.9–37.3, $n = 3$]) (Table 1); (2) head dorsally convex in lateral view; (7) tympanum concealed and only distinct anteroventrally; (3) eyes small, almost half the size of the eye-naris distance; (4) fingertips tapering, except on Finger IV that has a rounded tip; (5) subarticular tubercles not visible on fingers; (6) thenar tubercle large and prominent, palmar tubercle indistinct; (7) Fingers II and III with well-developed preaxial fringe extending towards the base of fingers, and Fingers I and II with narrow postaxial fringe in males and females; (8) toe tips slightly expanded; (9) inner and outer metatarsal tubercles indistinct; (10) dorsal color pattern medium brown with numerous small spots (orange in life, cream in preservative) forming a mottled pattern over the back and head with spots increasing in size towards the flanks, arms and legs, a more or less continuous stripe (often broken in small fleck/spots) extends from the snout along the canthus rostralis and upper eyelid to midway between eye and axilla; (11) venter pearl white with sparse melanophores, throat similarly colored as dorsum in males and females; (12) conspicuous depressions on the prootic and frontoparietal, sphenoid-nasal bridge and septum highly ossified, axis processes with enlarged terminals parts and atlas with a bulbous neural spine, phalanges I and II of Finger III shorter than metacarpal, tibiale and fibulare only fused on extremities; (13) call consisting in a pulsed note 0.282–0.366 s in length with a dominant frequency at 1.01–1.12 kHz ($n = 5$) (Fig. 8, Table 2).*S. ajuricaba* sp. nov. can be distinguished from *S. rabus* by considerably being larger (SVL = 29.3–37.3 mm in *S. ajuricaba* vs. 16.2–19.0 mm in *S. rabus*); in having smaller eyes (4.9% of SVL in *S. ajuricaba* vs. 7.3% in *S. rabus*); well-developed fringes on Fingers II and III (vs. no fringes in *S. rabus*); a convex head in lateral view (vs. flat in *S. rabus*); a brown dorsum with a mottled pattern (vs. uniformly dark brown in *S. rabus*); a call consisting of longer and pulsed notes (0.282–0.366 s in *S. ajuricaba* vs. 0.039 and tonal in *S. rabus*); and conspicuous depressions on the prootic and frontoparietal (inconspicuous in *S. rabus*) and tibiale and fibulare only fused on extremities (totally fused in *S. rabus*).*S. ajuricaba* sp. nov. can be distinguished from *S. salseri* in being larger (SVL = 29.3–33.2 mm in males of *S. ajuricaba* vs. 23.7–26.4 mm in males of *S. salseri*); in having smaller eyes (4.9% of SVL in *S. ajuricaba* vs. 5.4% in *S. salseri*); well-developed fringes on Fingers II and III (vs. rudimentary fringes in *S. salseri*); a convex head in lateral view (vs. flat in *S. salseri*); a brown dorsum with a mottled pattern (vs. sparse spots in *S. salseri*); a call consisting of longer and pulsed notes (0.282–0.366 s in *S. ajuricaba* vs. 0.079 and tonal in *S. salseri*); and conspicuous depressions on the prootic and frontoparietal (inconspicuous in *S. salseri*), axis processes with enlarged terminals parts (vs. not enlarged in *S. salseri*) and atlas with a bulbous neural spine (vs. not bulbous in *S. salseri*), phalanges I and II of Finger III shorter than metacarpal (vs. longer in *S. salseri*).*S. ajuricaba* sp. nov. can be distinguished from *S. mirandaribeiroi* in having Fingers II and III tapering with well-developed fringes (vs. fingertips rounded and less developed fringes in *S. mirandaribeiroi*); and a call consisting of longer notes with partly fused pulses (0.282–0.366 s and 12–16 partly fused pulses vs. 0.130–0.194 s and 5–8 entirely fused pulses in *S. mirandaribeiroi*).*S. ajuricaba* sp. nov. can be distinguished from *S. zombie* sp. nov. in being smaller (SVL = 29.3–33.2 mm in males of *S. ajuricaba* sp. nov. vs. 37.0–40.6 mm in males of *S. zombie* sp. nov.); in having a stripe along the canthus rostralis and upper eyelid extending between eye and axilla (stripe absent in *S. zombie* sp. nov.); and in having a call consisting of longer pulsed notes (0.282–0.366 s and 12–16 partly fused pulses vs. 0.147–0.167 s and tonal notes in *S. zombie*).*S. ajuricaba* sp. nov. can be distinguished from *S. mesomorphus* sp. nov. by being larger (SVL = 29.3–33.2 mm in males of *S. ajuricaba* sp. nov. vs. 22.9–26.0 mm in males of *S. mesomorphus* sp. nov.); in having a brown dorsum with a mottled pattern (vs. light to dark brown with sparse speckles and blotches in *S. mesomorphus* sp. nov.); a call consisting of longer pulsed notes, with 0.282–0.366 s and 12–16 partly fused pulses (0.160–0.173 s and tonal notes in *S. mesomorphus*); and conspicuous depressions on the prootic and frontoparietal (vs. inconspicuous in *S. mesomorphus*), phalanges I and II of Finger III shorter than metacarpal (vs. same size in *S. mesomorphus*).*3.1.5.5. Description of the holotype.* An adult female, 35.9 mm SVL; body stout; head slightly longer than wide, HL 18% of SVL; dorsal and ventral skin smooth; supratympanic fold running from the posterior corner of the eye, curving towards the axilla, continuous with an occipital (postcephalic) fold and a gular fold; presence of a thoracic fold; snout long and strongly protruding, projecting well beyond the end of the lower jaw (1.94 mm), rounded in dorsal and lateral view. Eyes small, 64% of EN; nares located laterally closer to the tip of the snout (1.3 mm) than to the eye (2.5 mm); canthus rostralis rounded, loreal region strongly concave, grooved; IN 34% of HW; EN 39% of HL. Tympanum concealed and only distinct anteroventrally, obscured posterodorsally by a supratympanic fold; choanae small (50% of ED), drop shaped, located anterolaterally, no odontophore.Forelimb robust, skin smooth; HAND 16% of SVL; Finger II longer than Finger I when fingers adpressed; fingers short, tips tapering, except on Finger IV that has a rounded tip, unwebbed, with pre- and postaxial fringes (except postaxially on Finger IV), particularly developed on Fingers II and III and extending towards the base of fingers; no finger discs; relative lengths of adpressed fingers III > IV > II > I; subarticular tubercles not visible on fingers; thenar tubercle large and prominent, palmar tubercle indistinct.Hind limb robust, skin smooth; TL 35% of SVL; FL34% of SVL; relative length of adpressed toes IV > III > V > II > I; Toe I very short, its tip reaching the base of Toe II when toes adpressed; toe without discs, Toes II, III and IV have slightly expanded tips. Toes unwebbed with narrow pre- and postaxial fringes. Subarticular tubercles not visible on toes; inner and outer metatarsal tubercle indistinct. Metatarsal fold absent.

3.1.1.47. Color of holotype in life Information not available.

3.1.1.48. Color of holotype in preservative Dorsum medium brown with numerous small cream spots forming a mottled pattern over the back and head with spots increasing in size towards the flanks, arms and legs, presence of a stripe along the canthus rostralis and upper eyelid that extends midway between eye and axilla. Venter pearl white with sparse melanophores, throat similar to the dorsum in color (Fig. 8).

3.1.1.49. Variation For morphometric variation see Table 1. Sexual dimorphism is apparent in the presence of a supracarpal pad in males, but dimorphism in body size remains subtle. Linea masculina visible in life through the translucent ventral skin in males. Ovaries are visible through the translucent skin in gravid females, and in preservative in females. Coloration varies little across specimens (Fig. 9).

3.1.1.50. Advertisement call Five specimens calling from underground galleries were recorded from a distance of about 2 m at air temperatures ranging from 22 to 24 °C (temperatures unknown in galleries). Descriptive statistics of call parameters are presented in Table 2. *S. ajuricaba* sp. nov. emits single pulsed notes (note length mean = 0.322, range 0.282–0.366 s) every 6.91 s on average (range 5.2–9.04 s). The spectral structure of the note has a developed harmonic structure and the fundamental (dominant frequency) is 1.06 kHz on average (range 1.01–1.12 kHz). These notes are composed of 12–16 partly fused pulses (ca. 0.02 s in length) of decreasing energy and with a downward fre-

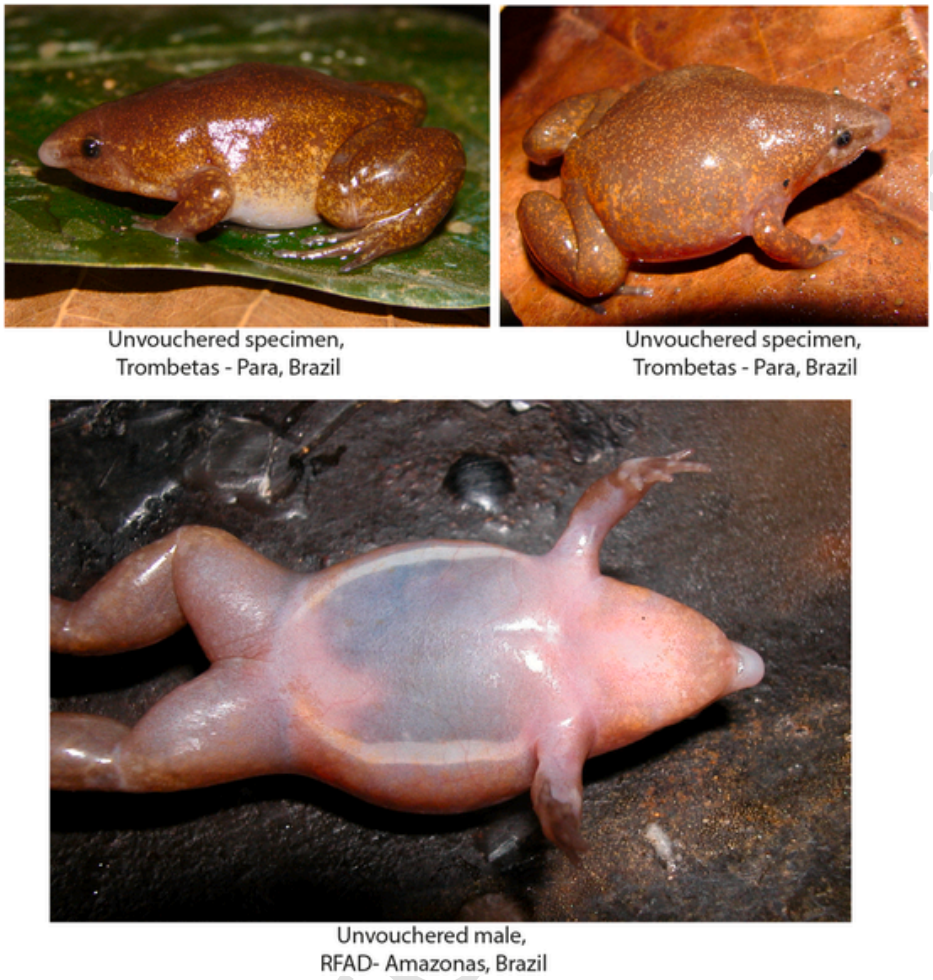

Fig. 9. Variation among specimens of *Synapturanus ajuricaba* sp. nov. (photo of the Trombetas specimens by Tiago Pezzuti, and of the unvouchered male from Reserva Florestal Adolpho Ducke by W.E. Magnusson and A.P. Lima).

quency between the beginning and the end of the note (ca. 0.05–0.09 kHz) (Fig. 8, Table 2).

3.1.1.51. Habitat and natural history This species occurs in pristine *terra firme* forest. Calling activity is mostly circumscribed during and after rain showers of November and December (Menin et al., 2008). Menin et al. (2007) provided detailed information about the reproduction and embryonic/larval development of this species from a population nearby Manaus, Brazil (under the name *Synapturanus* cf. *salseri*). Five clutches contained a mean of eight eggs; tadpoles hatched approximately at stage 42 of Gosner (1960). All clutches were found in burrows, approximately 5–10 cm below the soil surface and within 20 cm of an adult male (Menin et al., 2007). Pyburn (1975) found a downward curve at the end of the tail in *S. salseri* in stage 41. This characteristic was not observed in *S. ajuricaba* sp. nov. Moreover, the total length of *S. salseri* tadpoles at stage 41 from Colombia was much greater (23.7 mm, one individual) than that observed by Menin et al. (2007) in *S. ajuricaba* sp. nov. (12.6 ± 0.6 mm, n = 7). Vocalizations are commonly heard during the rainy season between November and May (Menin et al., 2008). We also report the presence of three ants in the stomach of one specimen (INPA-H11873 from Reserva Florestal Adolpho Ducke, Manaus, Amazonas state).

3.1.1.52. Etymology The specific name *ajuricaba* is used as a noun in apposition and is given as a reference to the legendary indigenous figure, Ajuricaba, a prominent leader of the Manaós indigenous people—considered extinct. They were one of the most important tribes of the Rio Negro. Ajuricaba led several incursions by the Manaós and allied groups against European settlements in the Rio Negro region. For his effort and leadership, he became one of the symbols of indigenous resistance against European colonization. Ajuricaba was eventually captured and was to be conducted to Belém, probably to be enslaved. History tells that during his transport to the capital, while still in chains, Ajuricaba and his men rebelled against captors, killing several of them. Eventually losing the battle, the survivors, including Ajuricaba, jumped into the waters of the Amazon river and were never seen again. For additional details about this important indigenous figure, see Souza (2019).

3.1.1.53. Distribution and conservation status This species is known from five localities (Ilha Sapupara, Trombetas, Floresta Nacional de Faro, Reserva Florestal Adolpho Ducke, Ponte Cacau Pereira) in the northern parts of the Amazonas and the Pará states, Brazil (Fig. 2). These populations range between 100 and 200 m asl.We suggest considering this species as Data Deficient according to the IUCN criteria (IUCN, 2020a,b).

3.2. Comparative osteology of Synapturanus

3.2.1. Ossification and preservation artefacts

Analyses of μCT-scans revealed a conspicuous variation in osteological characters within *Synapturanus*. We evaluated whether differences in ossification were consistent and inherent to each species or merely due to preservation artefacts by examining several adult specimens per

species. Juvenile specimens were all poorly ossified and therefore not used in the comparative analyses.

Although species in the genus can be overall considered hyperossified, some regions display variable degrees of ossification, partly due to (1) interspecific variation, (2) ontogenetic variation, and (3) preservation (e.g., decalcification after decades of preservation in alcohol and/or use of high formalin concentration for fixation). For example, cranial bones are generally fused forming a robust skull. However, the degree of fusion is variable as seen through suture lines that can be completely invisible in recently collected *S. mirandaribeiroi* (Fig. 10, MNHN-RA-2020.0084), visible as narrow grooves in *S.* sp. "Ecuador" (Fig. 10; Fig. S2) or clearly differentiated in the old paratype of *S. mirandaribeiroi* (Fig. 10, MNHN-RA-1974.0397). Other naturally less calcified bones, apparently prone to be affected by long-term preservation, are the lateral part of the prootic and the palatine region, which was previously mentioned as displaying variable ossification (Zweifel, 1986), the autopod, the neural spine and the ischium (urostyle). The paratype of *S. mirandaribeiroi* (MNHN-RA-1974.0397) is notably decalcified, likely because of its long-term preservation, and some characters like the sphenoid-nasal bridge are impossible to evaluate (Fig. 10; Fig. S2); the scapula and coracoid are differentiated while those bones are fused in other specimens; the proximal epiphysis of the humerus, femur, tibio-fibula and tarsum are not visible; metacarpal bone and prepollex are not visible either. The paratype of *S. salseri* is also slightly decalcified, e.g., the distal epiphysis of the femur and some metacarpal bones are not visible. One needs therefore to be careful when assessing the diagnostic value of these characters.

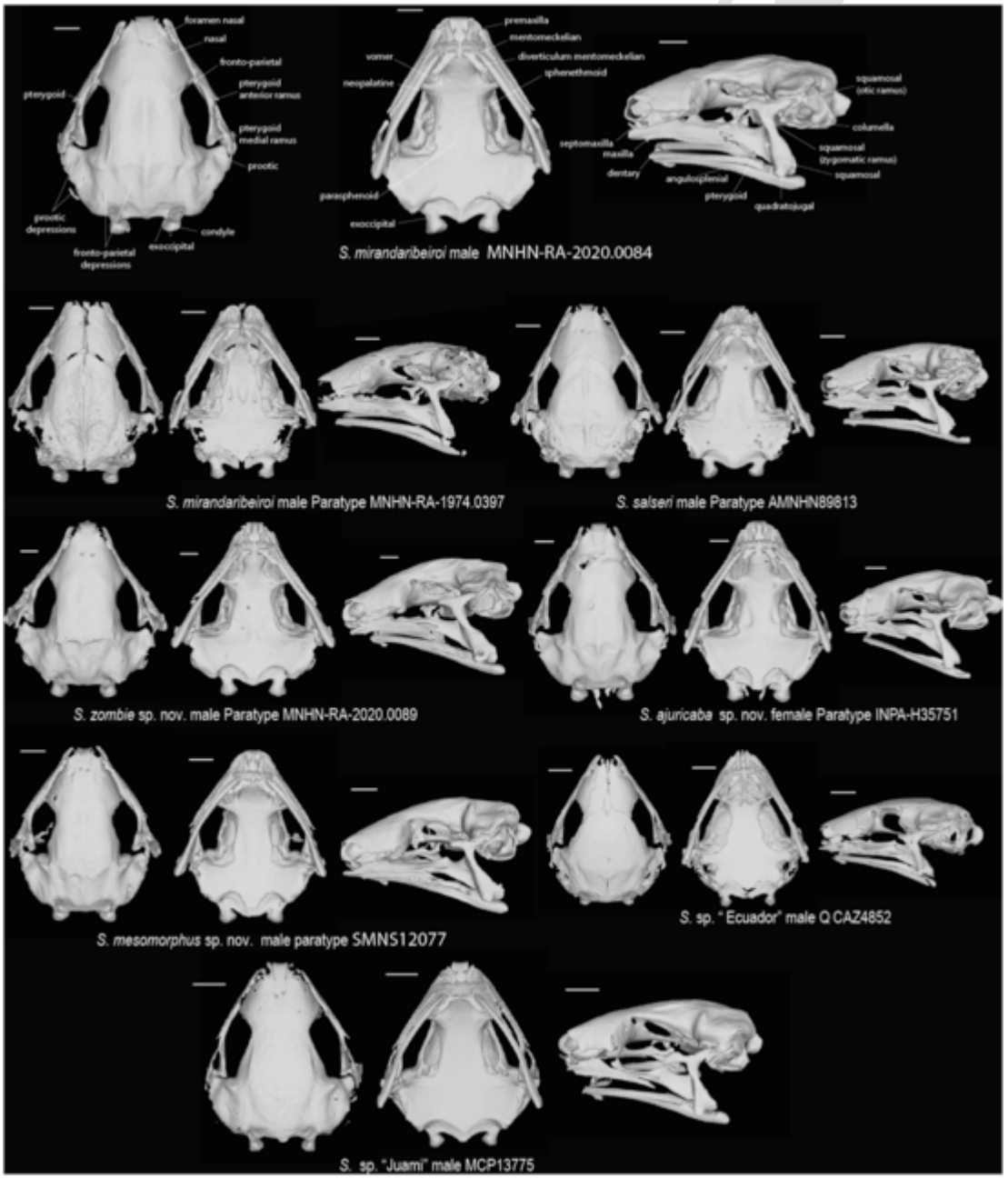

Fig. 10. Variation in the skull of *Synapturanus.* All species shown in dorsal (left), ventral (center) and lateral (right, skull in left side view) views. One mm scale bars are illustrated for each view.

3.2.2. Cranium

Skull robust and compact, convex in lateral view, projecting anteriorly, truncate or acuminate in dorsal view, slightly longer than wide. Most cranial bones are in contact but the degree of contact differs among specimens and can be categorized into three states, as suggested in Kok et al. (2020): (1) free, with no contact between structures (e.g., *S. mirandaribeiroi* MNHN-RA-1974.0397); (2) structures in contact with a visible suture line (e.g., *S.* sp. "Ecuador"); or (3) fused, structures in contact with a suture line being barely visible or absent (e.g., *S. zombie*) (Fig. 10). Nasal, sphenethmoid and frontoparietal are fused. The posterior end of the nasal is projecting laterally well beyond the anterior end of the frontoparietal, which is particularly visible when cranial bones are free (1) or with a visible suture line (2). Each nasal bone generally anteriorly perforated by a nasal foramen (often opening into the nasal cavity via a small canal). When present on both bones they are generally positioned asymmetrically (Fig. 10; Fig. S2). These foramina are highly variable among specimens and seem little informative to diagnose species. Nasal septum is dense enough to be visible. The nasal extends anteriorly, curving towards the sphenethmoid forming a strong arch protecting the nasal cavity. Partly calcified tissue is attached to the nasal as a protruding snout extending well beyond the lower jaw. The ontology of this nasal-sphenethmoid bridge is unclear and could either result from the extension of the sphenoid as suggested by Nelson & Lescure (1975) or/and chondrosis of the nasal region tissue. The *pars facialis* and lateral part of the nasal are not in contact.

The prootic region is well developed laterally, and is well ossified in all our specimens. Dorsal parts of the frontal and the prootic are sculpted with two shallow depressions each: at the level of the prootic/frontoparietal and in a medial position on the frontal, and laterally and medially on the prootic (Fig. 10; Fig. S2). Occipital condyles are ovoid and vertical. Prootic, sphenethmoid and exoccipital are ventrally fused to the parasphenoid, the degree of visibility of the suture line being variable from one specimen to another. Parasphenoid, sphenethmoid, and palatine are fused in most specimens (sphenethmoid seems to extend well beyond the palatine, as also observed in decalcified specimens). The palatine region is singular, bones are fused or closely in contact forming a robust structure; neopalatine is concave and in contact with the parasphenoid medially, the sphenethmoid dorsally, and the vomer anteriorly. Neopalatine fused with vomer in most specimens. Vomer consists of a thin vertical bony lamella parallel to the anterior–posterior axis of the skull.

The columella is medially enlarged. The squamosal is T-shaped with a slightly inflated base because of its fusion with the quadratojugal. The zygomatic ramus is slightly less developed and a little bit longer than the otic ramus in most specimens (roughly equal in length in *S. salseri* AMNH89813, more developed in *S. mesomorphus* sp. nov. SMNS12077 and *S. mirandaribeiroi* MNHN-RA-1974.0397). Incomplete pterygoid-prootic arch, but both pterygoid and prootic are practically in contact. Incomplete maxillary arch sensu Trueb (1973) which contradicts Nelson & Lescure (1975) and Walker (1973) but is in accordance with Carvalho (1954) and Zweifel (1986) who reported the quadratojugal and the maxilla not being in contact. Squamosal with a laterally inflated base which could be the quadratojugal, both forming a concavity where the angulospenial inserts. Well-developed pterygoid overlapping to half of the length of the maxilla(Fig. 10; Fig. S2). The anterior part of the pterygoid is imbricated into the maxilla. The posterior part of the pterygoid is firmly in contact with the medial ramus of the squamosal. Pterygoid body deep, slightly arched in dorsal view, bearing a mediodorsal tuberosity and a deep lateral groove; posterior and medial rami poorly differentiated. Maxillary well-developed, thicker near the nasal region, and protruding well beyond the mandible. The ventral part of the premaxilla is curved. The allary process of the premaxilla is long and inclined forward (angle between the base and the tip of the process ≈ 140°). Septomaxilla present, rounded ventrally and notched posteriorly.

The mandible is acuminate, slightly arched ventrally, posteriorly thicker, the dentary is slim and overlaps half the length of the angulosplenial, which extends slightly beyond the squamosal and the quadratojugal. Small mentomeckelians with the characteristic microhylid well-developed meckelian diverticulum, slightly longer than mentomeckelians, and parallel to the mandible.

3.2.3. Interspecific variation in cranial characteristics

Except from size differences among species (relative size: *S. zombie* sp. nov. (n = 2) > *S. ajuricaba* sp. nov. (n = 2) > *S. mirandaribeiroi* (n = 3) > *S. mesomorphus* sp. nov. (n = 4) > *S. salseri* (n = 1)), skull shape is overall conserved among species, with a few variable characteristics, nonetheless. The cranium of *Synapturanus* sp. "Ecuador" is substantially more elongated (HW < HL), less ossified, and more acuminate in dorsal view than in other *Synapturanus* species (cranium truncate or rounded in shape and cranial bones more heavily fused in the other species). *Synapturanus* sp. "Juami" has a rounded skull shape (vs. truncate in the species of the eastern clade), a shorter snout (the nasal bones do not extend laterally as in other species). *S. salseri* and *S. mesomorphus* sp. nov. differ from *S. mirandaribeiroi*, *S. zombie* sp. nov. and *S. ajuricaba* sp. nov. by having less conspicuous depressions on the prootic and frontoparietal. Sphenoid-nasal bridge and septum is more ossified in *S. mirandaribeiroi*, *S. zombie* sp. nov. and *S. ajuricaba* sp. nov. than in the other species (Fig. 10; Fig. S2). *Synapturanus* sp. "Ecuador" differs from other species by having a shorter medial ramus of the squamosal, a thickening of the top medial ramus region of the squamosal and a more developed otic ramus than the zygomatic ramus. *Synapturanus* sp "Juami" differs from other species by having a well-developed and shorter otic ramus with an arched and longer zygomatic ramus and by having the anterior part of the maxilla thicker than its posterior part. Furthermore the anterior part of the maxilla in S. sp. "Juami" doesn't extend beyond the premaxilla like in the other species (Fig. 11; Fig. S3).

3.2.4. Vertebrae

Nine vertebrae (eight presacral + one sacral); presacral vertebrae procoelous; eighth vertebra (V8) amphicoelous (Fig. 11; Fig. S3). Atlas and axis well sculpted and developed, axis with short transverse processes, distally enlarged. V3 transversal processes with a dorsal medial apophysis. The neural spine is bulbous in V1–2, with a ridge in V3–5 and smooth in V6–8. Sacral diapophyses rounded. Smooth ilia and urostyle. Urostyle ridge present, extending on ¾ of its length.

3.2.5. Interspecific variation in vertebral characteristics

Synapturanus sp. "Ecuador" differs from the other species by having a relatively small atlas (16 < HL/AL <17) being only slightly sculpted (cf. below). *Synapturanus* sp. "Juami" and *S. salseri* differ from *S. mesomorphus* sp. nov., *S. mirandaribeiroi*, *S. ajuricaba* sp. nov. and *S. zombie* sp. nov. by having a relatively medium-sized (12 < HL/AL < 13) and moderately sculpted atlas (Fig. 11; Fig. S3). *S. mesomorphus* sp. nov. differs from *S. mirandaribeiroi*, *S. ajuricaba* sp. nov. and *S. zombie* sp. nov. by having a moderately sculpted atlas despite sharing with them a relatively large atlas (8 < HL/AL < 10). In *S. mirandaribeiroi*, *S. ajuricaba* sp. nov. and *S. zombie* sp. nov., the atlas is larger and more developed with a bulbous neural spine and a depression on each side of the vertebral body, and the posterior neural arch bears a crest starting from the post zygapophysis, extending to the neural spine. Additionally, *S. salseri*, *S.* sp. "Juami" and *S.* sp. "Ecuador" differ from *S. mirandaribeiroi*, *S. zombie, S. ajuricaba* and *S. mesomorphus* by having an atlas with a longer axis process with no enlarged terminal part and shorter lateral processes of trunk vertebrae V–VIII. In *S. salseri* and *S.* sp. "Juami" the lateral processes are only slightly shorter while in *S.* sp

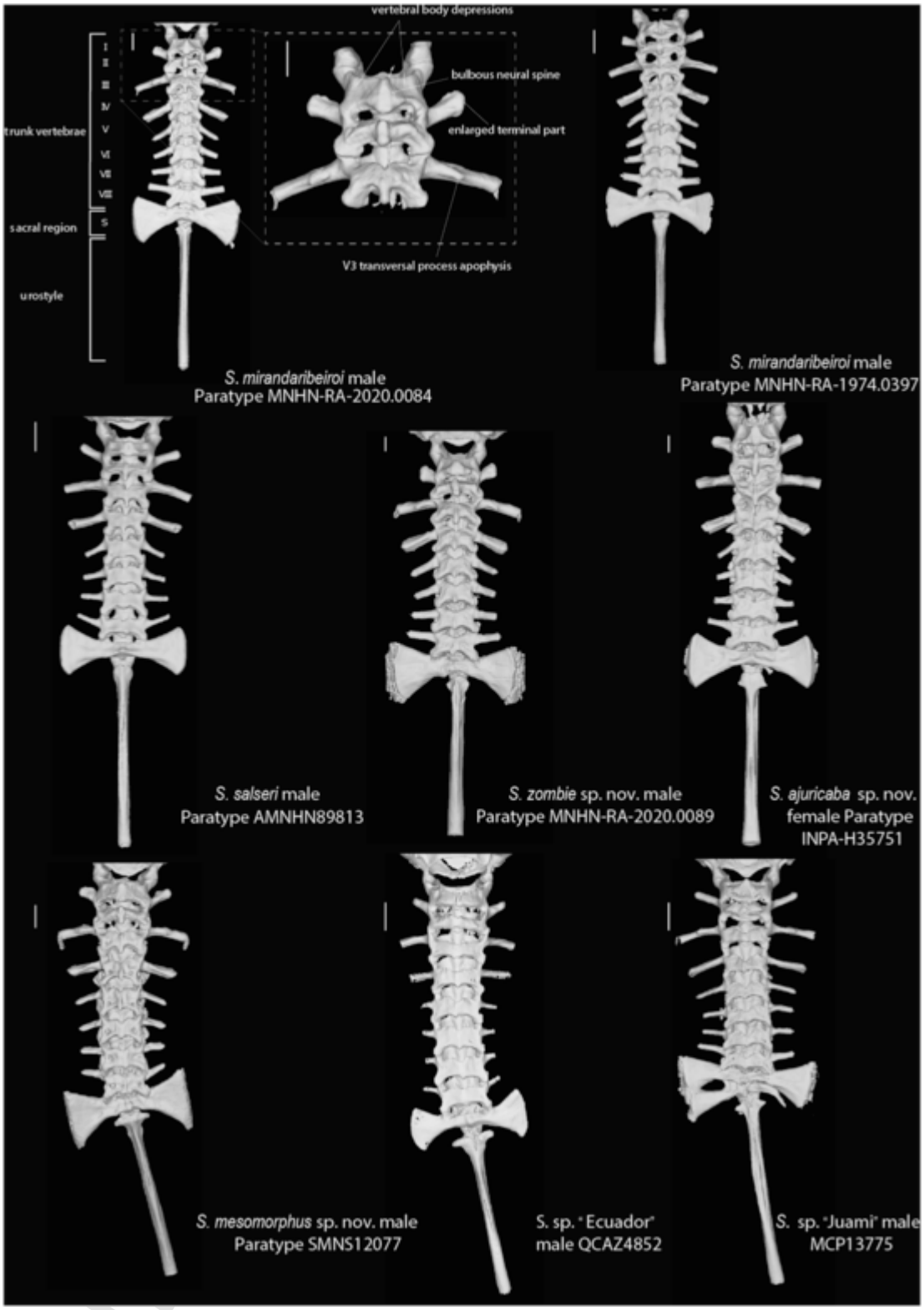

Fig. 11. Variation in the vertebral column of *Synapturanus.* All species shown in dorsal view. One mm scale bars are illustrated for each view.

"Ecuador" they are distinctly much shorter, being half of the length of the ones of *S. salseri* and *S*. sp "Juami" and less than half of the length of ones of other species.

Two specimens (SMNS12077 and SMNS12078) of *S. mesomorphus* have the sacrum with straight edges (vs. rounded in other species and in other *S. mesomorphus* specimens). MCP13775 (*S*. sp. "Juami") has a malformation on the left part of the sacrum (Fig. 11; Fig. S3).

3.2.6. Pectoral girdle

Base and anterior part of the suprascapula partially ossified. Clavicle absent (Fig. 12; Fig. S4). Scapula and coracoid completely fused

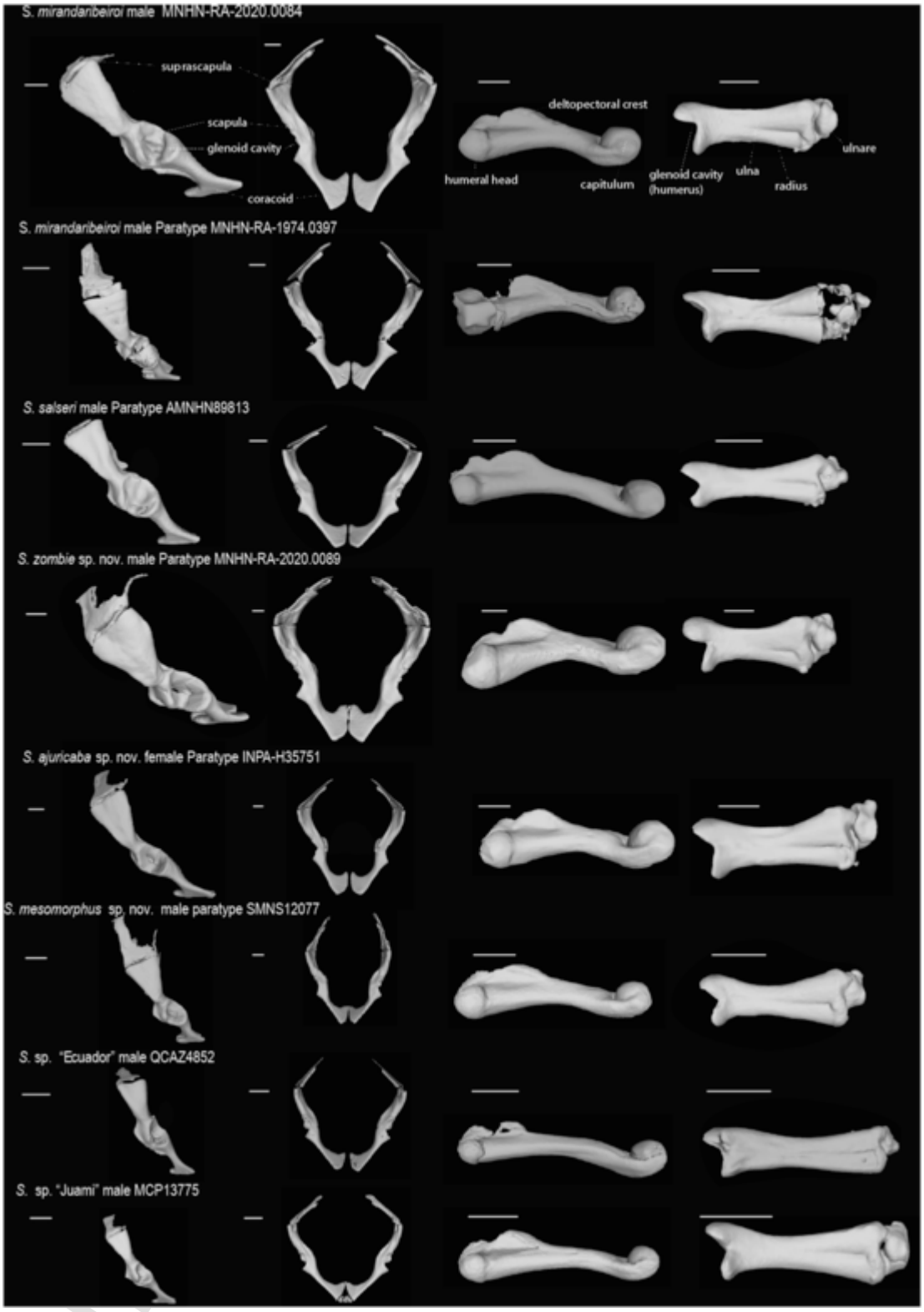

Fig. 12. Variation in the pectoral girdle elements of *Synapturanus.* From left to right, pectoral girdles shown in lateral, and frontal views, right humerus in dorsal view, right radio-ulna in dorsal view. One mm scale bars are illustrated for each view.

without evidence of suture except in two specimens: *S. ajuricaba* INPA-H38464 and *S. mirandaribeiroi* MNHN-RA-1974.0397. Short humerus associated with an enlarged deltopectoral crest. Short and thick radio-ulna. Ulna and radius well-developed, ulna thicker than radius (Fig. 12; Fig. S4). Prepollex present, composed of two bones, the proximal one is rounded, whereas the distal one is acuminate anteriorly (Fig. 13; Fig. S4). Element Y large, as big as the ulnare. Metacarpals and phalanges I and II distally enlarged. Terminal phalanges pointed.

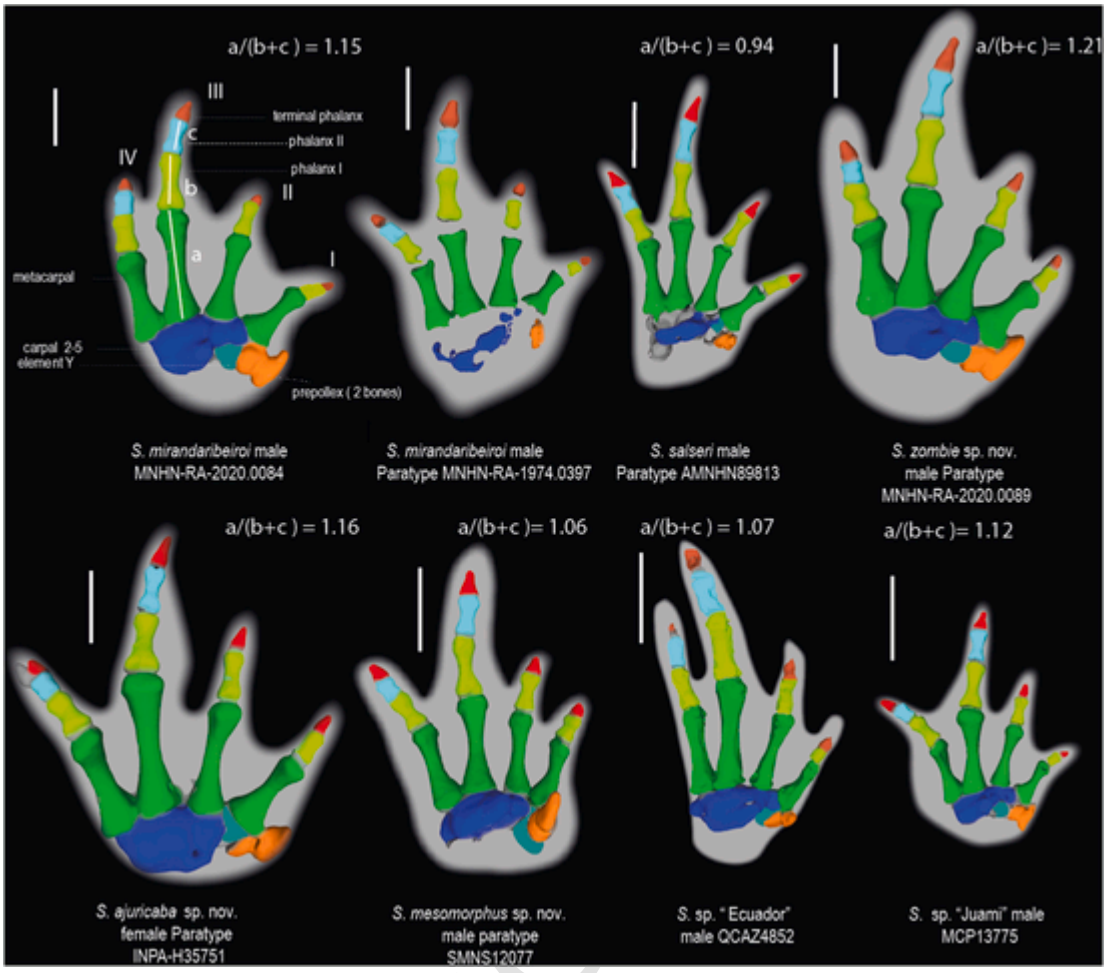

Fig. 13. Variation in hand morphology of *Synapturanus*. All species shown in ventral view. One mm scale bars are illustrated for each view. The additional structures appearing in grey behind the carpals when they are not totally preserved, correspond to the radiale, the intermedium, and the ulnare.

3.2.7. Interspecific variation in pectoral girdle

Synapturanus sp. "Ecuador" differs from the other species by having a lower ratio of humerus/radio-ulna length (ratio humerus/radio-ulna for *S*. sp. "Ecuador" H/R < 1.80 vs. constant among other species examined H/R ≈ 2). Radio-ulna is thus proportionally longer in *Synapturanus* sp. "Ecuador". Relative size of enlarged dectopectoral crest and capitulum as follows: *S. ajuricaba* sp. nov. > *S. zombie* sp. nov.> *S. mirandaribeiroi* > *S. mesomorphus* sp. nov. > *S. salseri* > *S.* sp. "Juami" > *S.* sp. "Ecuador" suggesting different modalities in fossoriality (Fig. 12; Fig. S4). Prepollex laterally protruding in *S. zombie* sp. nov., *S. ajuricaba* sp. nov., *S. mirandaribeiroi, S. mesomorphus* sp. nov. and *S. salseri* (vs. poorly developed in *S*. sp. "Ecuador and *S*. sp. "Juami"). Combined length of phalanges I and II of Finger III longer than metacarpals in *S. ajuricaba* sp. nov., *S. zombie* sp. nov. and *Synapturanus mirandaribeioi* (metacarpal length 115–125% of phalanges I + II vs. 94–112% in *S. mesomorphus* sp. nov., *S. salseri*, *S*. sp. "Juami" and *S*. sp. "Ecuador") (Fig. 13; Fig. S5). All these differences suggest more pronounced fossoriality.

3.2.8. Pelvic girdle

Tibio-fibula is the longest bone in the pelvic girdle, slightly longer than the femur (mean across all specimens F/TF = 0.92 (SD = 0.03)), femur and tibio-fibula smooth (Fig. 14; Fig. S6). Condyles of the femur and tibio-fibula slightly larger distally than proximally. Tarsal region well ossified. Prehallux present. Absence of crista femoralis in all species. Tarsal epiphysis well developed, distal tarsal bones relatively reduced in size compared to the prehallux/element Y; d3 is slender and d1–d2 are small, oval. Prehallux composed of two juxtaposed bones, the distal one is slender, the proximal one is rectangular lying on the element Y, which is well developed and thicker than d3.

3.2.9. Interspecific variation in pelvic girdle

Synpaturanus sp. "Ecuador" has a distinctly fused tibiale and fibulare (vs. fused only in distal and proximal apophyses in the other species) (Fig. 14; Fig. S6). This fusion is also present in the other species (*S. rabus* - R. Keeffe pers. com., *S*. sp. "Divisor", *S*. sp. "Ecuador") of the western clade and probably represent a synapomorphy for that clade. Despite this unique fusion, the pelvic girdle elements are generally similar among all examined *Synapturanus*.

4. Discussion

4.1. Species diversity in Synapturanus

The discovery of phenotypically differentiated unnamed species in Amazonia is far from surprising. Most studies that have explored the question of how many species exist in particular groups of amphibians (e.g., Gehara et al., 2014; Fouquet et al., 2016; Kok et al., 2017; Vacher et al., 2017; Jaramillo et al., 2020), including Microhylidae (e.g., Peloso et al., 2014; de Sá et al., 2020), have uncovered high numbers of unnamed species. In many cases, the initial recognition of diversity is based on genetic data (commonly based on a single or very

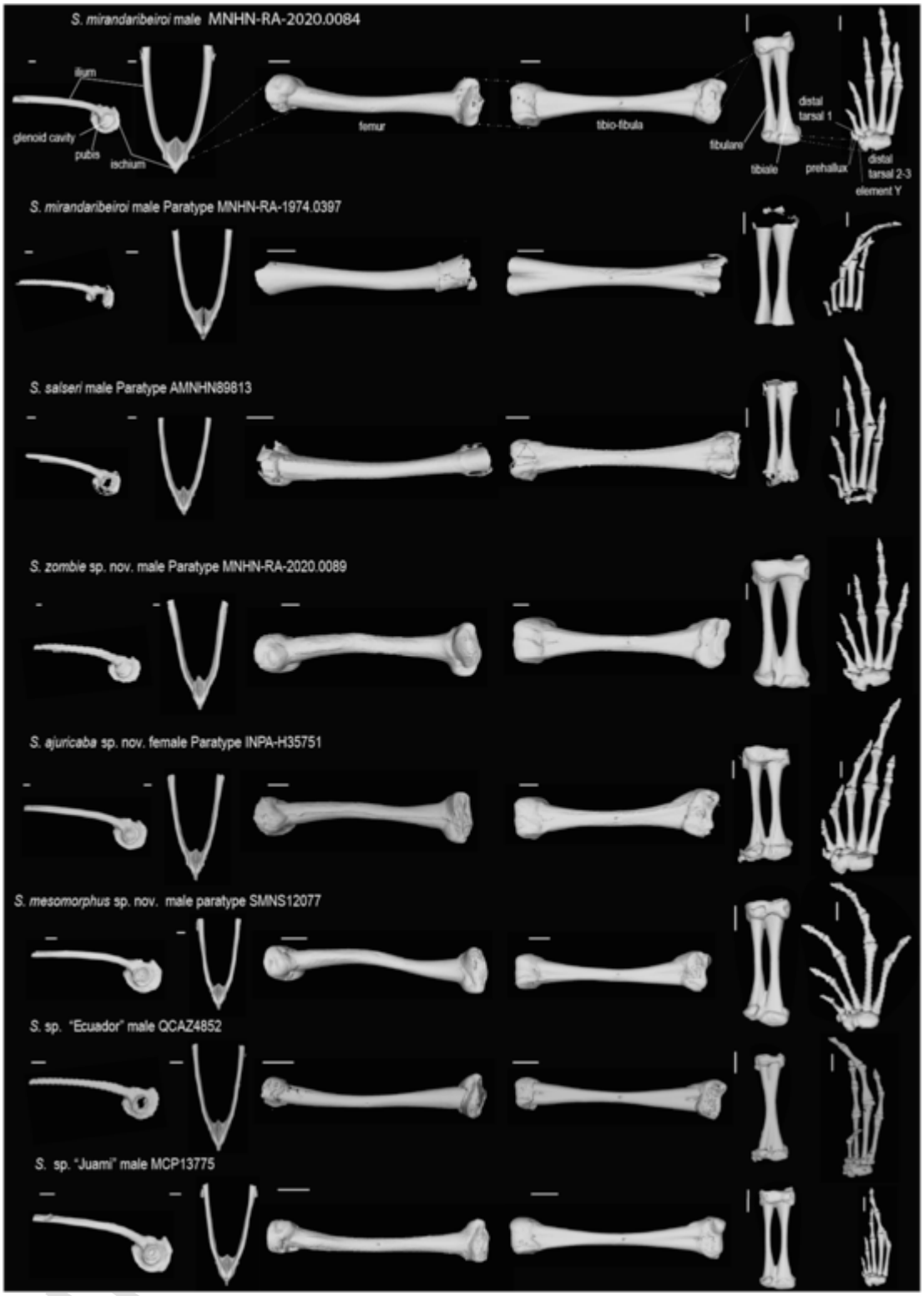

Fig. 14. Variation in the pelvic girdle elements of *Synapturanus*. From left to right, pelvic girdles shown in lateral, and ventral views, femur in dorsal view, tibio-fibula and foot morphology in ventral view. One mm scale bars are illustrated for each view.

few genes), but after closer examination most of the genetic lineages also present conspicuous phenotypic diagnostic characters (Peloso et al., 2014; Fouquet et al., 2013; Kok et al., 2016; Carvalho et al., 2021). Therefore, it is likely that many new taxa will continue to be discovered through the integrative use of DNA sequences and detailed phenotypic analyses, progressively unveiling the unknown diversity of Amazonian amphibians.

A recent DNA-based species delimitation work suggested that three to four times more species of frogs than formally recognized occur in Amazonia (Vacher et al., 2020). Moreover, a recent study targeted at uncovering the diversity within *Synapturanus* found 18 lineages that

could correspond to distinct species (Fouquet et al., 2021). These 18 lineages included 12 that were also phenotypically distinct (based on morphology and/or advertisement call data), and therefore recognized as *Confirmed Candidate Species* (CCS; Vieites et al., 2009). However, only three names were available for these candidate species within *Synapturanus*. The higher proportion of unnamed species in *Synapturanus* (six times) than in Amazonian frogs in general (four times) likely stems from the combination of the challenge in finding these secretive frogs (resulting is scarcity of specimens in collections and of natural history data), from the high regional endemism in the genus, and from the fact that the group has been taxonomically neglected for quite some time.

Herein, we named three of the species suggested as CCS by Fouquet et al., 2021, for a total of six formally recognized taxa in *Synapturanus*. There is, however, evidence suggesting that additional *Synapturanus* species may have not been included by Fouquet et al., 2021, most notably the large-bodied species from Colombia identified as *S. mirandaribeiroi* by Pyburn (1975). We also obtained call recordings from Rio Juruá and Novo Airão (Amazonas, Brazil) that display unique characteristics and deserve additional scrutiny. Finally, the conspecificity of the populations from French Guiana and Suriname identified as *S. mirandaribeiroi* with the ones from northern Amazonas in Brazil remains ambiguous considering acoustic differences.

Therefore, it seems that the more we gather material and information, the more candidate species are unveiled in *Synapturanus*. Extensive work remains to be undertaken to describe the extant diversity in this genus, which implies to sample additional populations and not only specimens but molecular, acoustic and natural history data. We hope that this new contribution will encourage and facilitate further species descriptions in this extremely interesting and intriguing genus.

4.2. Morphological evolution and fossoriality in Synapturanus

Fouquet et al., 2021 identified three distinct osteological phenotypes within *Synapturanus*, based on the morphology of the skull and humerus. One of these phenotypes (phenotype 3) is found in the easternmost species of the eastern clade, i.e., the clade that includes *S. mirandaribeiroi*, *S. zombie*, *Synapturanus hades*, and two other candidate species south of the Amazon River. *S. salseri*, *S. mesomorphus* and another candidate species (*S.* sp. "Neblina") are distributed more westward and display a somewhat intermediate phenotype (phenotype 2), even though these species are included in the eastern clade. The examination of external and osteological variation across species as presented herein, led us to further characterize morphological evolutionary trends that are likely linked to behavioral differences across species, notably differences in fossoriality.

Reinforcement of the skull and the humerus in the species with phenotype 3 was previously identified in Fouquet et al., 2021. This trend is also evident in various additional structures examined herein, notably the atlas, the scapula-coracoid and the radio-ulna. The atlas and the posterior part of the head are strongly sculpted and the scapula-coracoid and radio-ulna are distinctly thicker in *S. hades*, *S. zombie* and *S. mirandaribeiroi*. These features could be linked with the insertion of larger muscles. The fusion of the scapula and the coracoid have been reported in several lineages of frogs. Notably, in the fossorial *Hemisus* (Engelkes et al., 2020) and in the semifossorial *Hamptophryne* (de Sá & Trueb, 1991) and may provide a strong, fixed arch against which the muscles of the shoulder and arm brace to enable digging. These characteristics are seemingly accompanied by a reduction of the size of phalanges, more developed fringes on the fingers, smaller eyes and an increase in body size, altogether suggesting an overall increase of the fossorial habits of these species (Emerson, 1976; Mendoza et al., 2020; Thomas et al., 2020). In contrast, the differences in the posterior part of the body are subtle among all *Synapturanus* species. In the absence of behavioral observations, and thus on the sole basis of morphology, it remains speculative to discuss the nuances in the digging behavior across species. Nevertheless, it seems very likely that all *Synapturanus* dig head-first. We also speculate that the easternmost species (associated with phenotype 3) have reinforced anterior bones and modified soft tissue on hand and snout compared to the other species either because they dig deeper, longer galleries, or simply because they spend more time underground or because the soil where they occur is mechanically more challenging to dig in. These hypotheses are not mutually exclusive, and need to be corroborated or rejected by actual field or laboratory observations.

Although meager, existing field observations suggest behavioral differences among the species having these distinct phenotypes. Western species, including *S. mesomorphus* and *S. salseri*, seem to be more epigean and have been more frequently observed exposed on the ground surface, either foraging or migrating for breeding. They were also collected with high success using pitfall trapping. In comparison, we have never seen a single specimen of *S. mirandaribeiroi*, *S. ajuricaba* or *S. zombie* above the ground surface. More fossorial habits in these easternmost species are corroborated by very short calling activity vs. apparently more prolonged and opportunistic calling activity observed in *S. salseri*, *S. mesomorphus* and *Synapturanus* spp. of the western clade. As far as we know, calling is circumscribed to a few hours during rain showers preceding the rainy season (November–December) in *S. zombie*.

An additional observation is that we often found female specimens while digging in search of calling males in this group of species. We thus hypothesized female vocalization and/or the possibility of reproductive fidelity over long periods and biparental care, a rare mating system in frogs (de Sá et al., 2020). Since we can reasonably speculate that finding a mate requires migrating at the surface in *Synapturanus*, the cost of such movements for reproduction may be reduced by reproductive fidelity. We additionally note that sexual dimorphism is very subtle in these easternmost species. In comparison, body size and proportion differences in the species of the western and central clades are conspicuous. This may also be the consequence of both sexes being fossorial in the easternmost species with both male and female digging galleries and foraging underground whereas this behavior may be different among sexes in western species. The limited data available on the diet of *S. ajuricaba* (herein), *S. salseri* (Pyburn, 1975), *S. rabus* (Pyburn, 1977), *S. mirandaribeiroi*, *S. mesomorphus* (Nelson & Lescure, 1975) suggest myrmecophagy in the entire genus that could take place either underground or above the ground surface, thus not providing more insight on the matter of degree of fossoriality.

The species forming the western clade (including *S. rabus*) share phenotype 1, characterized by a slender cranium and humerus (Fouquet et al., 2021). These species are also the smallest, and Pyburn (1977) noticed that they also display comparatively larger eyes than other species. They have been hypothesized to be the most epigean. In this paper we only thoroughly examined one of the candidate species included in that clade (*S.* sp. "Ecuador") for comparison with the newly described species. However, it is noteworthy that all species of the western clade examined in Fouquet et al., 2021 share a fusion of the tibiale and fibulare throughout their entire lengths to form a fused bone structure. This condition is only found in several Centrolenidae genera (Guayasamin et al., 2009) and in Pelodytidae (Sanchiz et al., 2002) (see also Duellman and Trueb, 1994), two families that are not fossorial and display high jumping performances. This fusion may thus confer the *Synapturanus* of the western clade strong jumping abilities related to their leaf-litter habitat (Fabrezi et al., 2017). Mendoza et al. (2020) found that jumping power declines more rapidly with body mass in burrowing species of frogs than non-burrowing species and suggested the existence of a functional trade-off between jumping and burrowing performance. Therefore, the smaller size of these species

compared to the ones of the eastern clade also strengthens the idea that they are more epigean.

Declaration of competing interest

The authors declare that they have no known competing financial interests or personal relationships that could have appeared to influence the work reported in this paper.

Acknowledgments

This study benefited from 'Investissement d'Avenir' grants managed by the Agence Nationale de la Recherche (CEBA, ref. ANR-10-LABX-25-01; TULIP, ref. ANR-10-LABX-41; ANR-11-IDEX-0002-02) and from the French Foundation for Research on Biodiversity (FRB) and its partners (https://www.fondationbiodiversite.fr/PMAST-SOR-2018-4). We also acknowledge additional support from Conselho Nacional de Desenvolvimento Científico e Tecnológico (PQ 302501/2019-3 granted to PLVP, CNPq #305617/2020-6 granted to MM), from Fundação de Amparo à Pesquisa do Estado de São Paulo (FAPESP # 2003/10335-8 and 2011/50146-6 granted to MTR), from Fonds voor Wetenschappelijk Onderzoek (FWO12A7614N and FWO12A7617N granted to PJRK), and from German Academic Exchange Service (DAAD) and Deutsche Forschungsgemeinschaft (DFG; ER 589/2-1 granted to RE). Permission to conduct biodiversity research in Guyana was provided by the EPA Guyana under research permit number 180609 BR 112, and fieldwork was made possible through the Iwokrama International Centre for Rain Forest Conservation and Development particularly R. Thomas and the forestry department of the Guyana Forestry Commission (GFC-PRDD). We are grateful to the Parc Amazonien de Guyane for having organized the field work on Mont Itoupé in 2016 and 2018 as well as to the Muséum National d'Histoire Naturelle and ProNatura international for having organized the "Our Planet Revisited" expedition on the Mitaraka Massif (with support from Conseil régional de Guyane, Conseil général de Guyane, FEDER funds, Parc Amazonien de Guyane, and DEAL Guyane. We also thank the Natuurbeheer and STINASU for allowing fieldwork in Suriname. For helping with access to specimens and pictures we would like to warmly thank Fernanda Werneck and Ariane Silva (INPA), Mark Wilkinson (BMNH), Jerome Courtois and Annemarie Ohler (MNHN), Gregory Pandelis (UTA); Addison Wynn (USNM), Taran Grant and Renato Recoder (MZUSP), Ana Prudente (MPEG), Darrel Frost, David Kizirian and David Dickey (AMNH), Alexander Kupfer (SMNS). The 3D data acquisitions were performed using the microcomputed tomography facilities of the magnetic resonance imaging platform member of the national infrastructure France-BioImaging [supported by the French National Research Agency (ANR-10-INBS-04, 'Investments for the future') and by the Labex CEMEB (ANR-10-LABX-0004) and NUMEV (ANR-10-LABX-0020) thanks to Renaud Lebrun. We also thank the American Museum of Natural History's Microscopy and Imaging Facility (H. Towbin and M. Hill) for help with acquiring and processing CT images. Field work benefited from the contributions of B. Villette, S. Marques de Souza, J. Dias Lima, S. Barrioz, M. Blanc, P. Gaucher, R. Jairam, P. Ouboter, S. Cally, J. Dias Lima. We are indebted to J. Lescure (MNHN), David Blackburn, Anthony Herrel, Rachel Keeffe for sharing information on specimens and frog morphology, as well as to W.E. Magnusson and A. P. Lima for sharing photos of specimens of *Synapturanus* in life. Finally, we warmly thank Mark D. Scherz and an anonymous reviewer for constructive comments that improved the clarity of our manuscript.

Appendix E. Supplementary data

Supplementary data to this article can be found online at https://doi.org/10.1016/j.jcz.2021.05.003.

Appendix A. Museum acronyms

MZUSP: Museum of Zoology of the University of São Paulo, Brazil; AMNH: American Museum of Natural History, USA; MNHN-RA: The reptiles and amphibians collection (RA) of the Muséum national d'Histoire Naturelle, France; UMMZ: University of Michigan Museum of Zoology, USA; INPA: Instituto Nacional de Pesquisas da Amazônia, Brazil; UTA: Herpetological Collections at the University of Texas at Arlington, USA; USNM: Smithsonian Institution, National Museum of Natural History, USA; ANDES: Universidad de los Andes, Colombia; MTD: Museum of Zoology Senckenberg Dresden, Germany; SMNS: State Museum of Natural History Stuttgart, Germany; RBINS: Royal Belgian Institute of Natural Sciences, Belgium; MPEG: Museu Paraense Emílio Goeldi, Brazil; CM: Carnegie Museum, USA; UT: University of Texas at Austin, USA; QCAZ: Museo de Zoología de la Pontificia Universidad Católica del Ecuador; Ecuador; MCP: Museu de Ciências e Tecnologia da Pontifícia Universidade Católica do Rio Grande do Sul, Brazil.

Appendix B. Additional material examined

Synapturanus mirandaribeiroi

Non type specimens (16 specimens).

MNHN-RA-2020.0079 (AF2791) MNHN-RA-2020.0080 (AF2844) MNHN-RA-2020.0082 (AF3975) three males from Mitaraka (2.2358°N 54.4493°W); MNHN-RA-2020.0081 (AF2845); MNHN-RA-2020.0083 (AF3732) and MNHN-RA-2020.0084 (AF3758) a female and two males from Voltzberg, Suriname; INPA-H10890, INPA-H11837, INPA-H11843, INPA-H11867, INPA-H13169, INPA-H13170, INPA-H19781, seven males from Reserva Florestal Adolpho Ducke (2.9661°S 59.9312°W); INPA-H34023 a male from Mata Goiabinha Av. das Torres (2.9610°S 60.0037°W); INPA-H18572 a female from Parque Estadual Rio Negro Setor Sul (2.7255°S 60.4045°W); INPA-H37891 a female from Assentamento Rio Pardo (1.7092°S 60.4387°W).

Synapturanus sp. "Timbo"

UTA-A-3987 (Photos by Gregory Pandelis) and UTA-A-4009 (Photos by Gregory Pandelis), two males from Timbo, Vaupes, Colombia.

Synapturanus mesomorphus

Non type specimens.

RBINS15790 (PK3513), a male collected by M. Wilkinson, D. Gower and P.J.R. Kok on the 17th of March 2011 in Iwokrama Forest Reserve, Guyana (4.3302°N 58.7984°W); RBINS15810, RBINS15813 (PK3544, PK3547), two males collected by M. Wilkinson, D. Gower and P.J.R. Kok on the 21st of March 2011 in Iwokrama Forest Reserve, Guyana (4.3302°N 58.7984°W); RBINS15789 (PK3512), a female collected by M. Wilkinson, D. Gower and P.J.R. Kok on the 17th of March 2011 in Iwokrama Forest Reserve, Guyana (4.3302°N 58.7984°W); RBINS15812 (PK3546), a female collected by M. Wilkinson, D. Gower and P.J.R. Kok on the 21st of March 2011 in Iwokrama Forest Reserve, Guyana (4.3302°N 58.7984°W); PK3789 (uncatalogued), a juvenile collected by J. Pinto and P.J.R. Kok on the 30th of November 2012 in Iwokrama Forest Reserve, Guyana (4.4128°N 58.7840°W); MW11578 a male and MW11576–77, MW11579 three females collected by M. Wilkinson, D. Gower and P.J.R. Kok on the 1st of March 2011 at Iwokrama (4.6714°N 58.6850°W), Guyana.

Appendix C. µCT-scans reference numbers

Taxon	Specimen voucher (Field N°)	Sex	Source (www.morphosource.org/Detail/MediaDetail/Show/media_id)
Synapturanus salseri	AMNH89813 paratype	M	M55253
Synapturanus mirandaribeiroi	MNHN-RA-1974.0397 paratype	M	M82442
Synapturanus mirandaribeiroi	MNHN-RA-2020.0081 (AF2845)	F	M82487
Synapturanus mirandaribeiroi	MNHN-RA-2020.0084 (AF3758)	M	M82490
Synapturanus zombie	MNHN-RA-2020.0089 (AF3723)	M	M82491
Synapturanus zombie	MNHN-RA-2020.0087 (AF3573)	F	M82495
Synapturanus sp. "Ecuador"	QCAZA2103	F	M83013
Synapturanus sp. "Ecuador"	QCAZA4852	M	M83016
Synapturanus mesomorphus	SMNS12077	M	M82497
Synapturanus mesomorphus	MTD48012	F	M82498
Synapturanus sp. Juami	MCP13775	M	M83885
Synapturanus sp. Juami	MCP13777	F	M83823
Synapturanus ajuricaba	INPA-H38464	F	M82659
Synapturanus ajuricaba	INPA-H35751	F	M82658

Appendix D. Morphometric data for each specimen

Specimen voucher (field N°)	Species	SEX	SVL	HL	HW	IO	IN	EN	ED	F
INPA-H18572	*S. mirandaribeiroi*	F	28.6	5.92	6		3.81	1.9	2.03	1.45
INPA-H37891 (HT8357)	*S. mirandaribeiroi*	F	31.56	6.01	5.8		3.35	2.13	2.22	1.3
MNHN-RA-2020.0081 (AF2845)	*S. mirandaribeiroi*	F	34.42	6.35	7.63		4.14	1.99	2.04	1.6
INPA-H13170	*S. mirandaribeiroi*	M	26.6	5.59	6.28		3.5	1.85	2.03	1.45
MNHN-RA-1974-397	*S. mirandaribeiroi*	M	26.67	5.17	4.85		3.31	1.68	1.73	1.62
INPA-H34023	*S. mirandaribeiroi*	M	27.16	5.36	5.86		3.5	1.67	1.88	1.53
INPA-H13169	*S. mirandaribeiroi*	M	28.33	5.65	6.35		3.89	2.08	2.11	1.5
MNHN-RA-2020.0079 (AF2791)	*S. mirandaribeiroi*	M	29.52	6.47	6.4		3.89			1.99
INPA-H19781	*S. mirandaribeiroi*	M	29.57	5.8	6.18		3.84			1.91
MNHN-RA-2020.0083 (AF3732)	*S. mirandaribeiroi*	M	29.68	5.77	5.93		3.6			1.79
INPA-H11837	*S. mirandaribeiroi*	M	29.88	5.17	5.7		3.6			1.95
INPA-H10890	*S. mirandaribeiroi*	M	29.9	5.47	6.29		3.68			1.93
MNHN-RA-2020.0084 (AF3758)	*S. mirandaribeiroi*	M	29.96	6.27	6.1		3.86			2.04
INPA-H11867	*S. mirandaribeiroi*	M	30.7	5.93	6.38		3.54			1.96
MNHN-RA-2020.0080 (AF2844)	*S. mirandaribeiroi*	M	30.78	6.17	6.45		4.02			1.89
MZUSP 159220 (MTR24135)	*S. zombie*	F	38.95	6.93	7.7		4.55			2.52
MNHN-RA-2020.0085 (AF0525)	*S. zombie*	F	42.12	7.14	7.73		4.86			2.43
MNHN-RA-2020.0087 (AF3573)	*S. zombie*	F	38.73	7.69	7.44		4.7			2.16
MNHN-RA-2020.0091 (AF3986)	*S. zombie*	M	37.01	7.28	7.17		4.43			2.47
MNHN-RA-2020.0090 (AF3985)	*S. zombie*	M	39.34	7.43	7.39		4.63			2.5
MNHN-RA-2020.0088 (AF3722)	*S. zombie*	M	40.24	7.34	7.5		4.9			2.6
MNHN-RA-2020.0089 (AF3723)	*S. zombie*	M	40.62	7.37	7.82		5.12			2.28
(MW11579)	*S. mesomorphus*	F	27.08	5.05	5.35		3.12			1.59
USNM588793 (BPN3762)	*S. mesomorphus*	F	27.35	5.68	5.85		3.67			1.73
(MW11576)	*S. mesomorphus*	F	27.39	5.33	5.26		3.15			1.85
USNM566235	*S. mesomorphus*	F	27.54	6.29	5.75		3.63			1.89
MTD49061	*S. mesomorphus*	F	28.41	4.71	5.63		3.04			1.53
(MW11577)	*S. mesomorphus*	F	28.7	5.34	5.11		3.33			1.79
MTD48012	*S. mesomorphus*	F	29.35	5.93	6.5		3.08			1.91
PK 1641	*S. mesomorphus*	F	29.27	5.42	5.91		3.23			1.72
PK 1396	*S. mesomorphus*	F	26.29	5.08	5.25		2.98			1.31
PK 1137	*S. mesomorphus*	F	26.51	4.75	5.17		3.15			1.4
PK 1143	*S. mesomorphus*	F	28.55	5.07	5.09		3.02			1.24
USNM588794 (BPN3813)	*S. mesomorphus*	M	23	5.01	5.06		3.14			1.66
(MW11578)	*S. mesomorphus*	M	24.95	4.92	5.12		3.11			1.83
SMNS12078	*S. mesomorphus*	M	25.4	4.81	5.25		2.95			1.71
SMNS12077	*S. mesomorphus*	M	25.95	5.09	5.47		2.92			1.81
PK 1397	*S. mesomorphus*	M	26.04	5.27	4.77		3.13			1.35

PK 1577	*S. mesomorphus*	M	22.88	4.37	4.9	2.89	1.18
INPA-H38464	*S. ajuricaba*	F	35.91	6.47	7.03	4.23	2.4
INPA-H28519	*S. ajuricaba*	F	36.27	6.34	7.3	4.3	2.34
INPA-H35751	*S. ajuricaba*	F	37.3	6.2	6.7	4.26	2.64
MPEG29453 (CN370/ PT-006)	*S. ajuricaba*	M	29.3	6	6	3.6	1.8
MPEG29457	*S. ajuricaba*	M	31.6	5.9	5.8	3.5	1.8
MPEG29456	*S. ajuricaba*	M	32.2	6.4	6.5	3.8	2.1
MPEG29454 (CN373/ PT-007)	*S. ajuricaba*	M	32.9	6.2	5.9	3.9	2.1
MPEG29458	*S. ajuricaba*	M	33.2	6.2	6.6	3.8	1.9

Uncited section

Dezé cache et al., 2017

References

Audacity TeamAudacity(R): free audio editor and recorder [computer application]Version 2.4.2 retrieved Sep 20th 2020 fromhttps://audacityteam.org/2020

Ávila-Pires, T.C.S.D., Hoogmoed, M.S., Rocha, W.A.D., 2010. Notes on the vertebrates of northern Pará, Brazil: a forgotten part of the Guianan Region, I. Herpetofauna. Bol. Mus. Para. Emilio Goeldi 5 13–11.

Barrio-Amorós, C.L., Brewer-Carías, C., 1999. Geographic distribution: *Synapturanus mirandaribeiroi*. Herpetol. Rev. 30, 51.

Barrio-Amorós, C.L., Brewer-Carías, C., Fuentes-Ramos, O., 2011. Aproximación preliminar a la herpetocenosis de un bosque pluvial en la sección Occidental de la Sierra de Lema, Guyana Venezolana. Rev. Ecol. Latinoam. 16, 1–46.

Barrio-Amorós, C.L., Rojas-Runjaic, F.J.M., Señaris, J.C., 2019. Catalogue of the amphibians of Venezuela: illustrated and annotated species list, distribution, and conservation. Amphib. Reptile Conserv. 13, 1–198.

Boulenger, G.A., 1882. Catalogue of the Batrachia Salientia S. Ecaudata in the Collection of the British Museum. second ed. Taylor and Francis, London.

Boulenger, G.A., 1900. Batrachians. In: Lankester, E.R. (Ed.), Report on a Collection Made by Messrs. F. V. McConnell and J. J. Quelch at Mount Roraima in British Guiana. Transactions of the Linnean Society of London. 2nd Series, Zoology, 8. pp. 55–56.

Carvalho, A.L. de, 1954. A preliminary synopsis of the genera of American microhylid frogs. Occas. Pap. Museu. Zool. 555, 1–19 University of Michigan.

Carvalho, T.R., Moraes, L.J., Lima, A.P., Fouquet, A., Peloso, P.L., Pavan, D., Drummond, L.O., Rodrigues, M.T., Giaretta, A.A., Gordo, M., Neckel-Oliveira, S., 2021. Systematics and historical biogeography of Neotropical foam-nesting frogs of the *Adenomera heyeri* clade (Leptodactylidae), with the description of six new Amazonian species. Zool. J. Linn. Soc. 191, 395–433.

Cole, C.J., Townsend, C.R., Reynolds, R.P., MacCulloch, R.D., Lathrop, A., 2013. Amphibians and reptiles of Guyana, South America: illustrated keys, annotated species accounts, and a biogeographic synopsis. Proc. Biol. Soc. Wash. 125, 317–578.

de Sá, R.O., Trueb, L., 1991. Osteology, skeletal development, and chondrocranial structure of *Hamptophryne boliviana* (Anura: Microhylidae). J. Morphol. 209, 311–330.

de Sá, F.P., Consolmagno, R.C., Muralidhar, P., Brasileiro, C.A., Zamudio, K.R., Haddad, C.F., 2020. Unexpected reproductive fidelity in a polygynous frog. Sci. Adv. 6 (33), eaay1539.

Dewynter, M., Courtois, A.E., Villette, B., 2019. La base de données Faune-Guyane. Amphibiens et Reptiles 2018 : première synthèse. 294p.

Dezécache, C., Faure, E., Gond, V., Salles, J.M., Vieilledent, G., Hérault, B., 2017. Gold-rush in a forested El Dorado: deforestation leakages and the need for regional cooperation. Environ. Res. Lett. 12, 034013.

Emerson, S.B., 1976. Burrowing in frogs. J. Morphol. 149, 437–458.

Engelkes, K., Kath, L., Kleinteich, T., Hammel, J.U., Beerlink, A., Haas, A., 2020. Ecomorphology of the pectoral girdle in anurans (Amphibia, Anura): shape diversity and biomechanical considerations. Ecol. Evol. 10, 11467–11487.

Ernst, R., Rödel, M., Arjoon, D., 2005. On the cutting edge-the anuran fauna of the Mabura Hill Forest Reserve, central Guyana. Salamandra 41, 179.

Ernst, R., Linsenmair, K.E., Rödel, M.O., 2006. Diversity erosion beyond the species level: dramatic loss of functional diversity after selective logging in two tropical amphibian communities. Biol. Conserv. 133 (2), 143–155.

Fabrezi, M., Alberch, P., 1996. The carpal elements of anurans. Herpetologica 52, 188–204.

Fabrezi, M., Goldberg, J., Chuliver Pereyra, M., 2017. Morphological variation in anuran limbs: constraints and novelties. J. Exp. Zool. B Mol. Dev. Evol. 328, 546–574.

Fitzinger, L.J.F.J., 1843. Systema Reptilium. Fasciculus Primus. Braumüller et Seidel, Wien.

Fouquet, A., Leblanc, K., Framit, M., Réjaud, A., Rodrigues, M.T., Castroviejo-Fisher, S., Peloso, P.L.V., Prates, I., Manzi, S., Suescun, U., Baroni, S., Moraes, L.J.C.L., Recoder, R., de Souza, S.M., Dal Vecchio, F., Camacho, A., Guellere, J.M., Rojas-Runjaic, F.J.M., Gagliardi-Urrutia, G., de Carvalho, V.T., Gordo, M., Menin, M., Kok, P.J.R., Hrbek, T., Werneck, F.P., Crawford, A.J., Ron, S.R., Mueses-Cisneros, J.J., Rojas Zamora, R.R., Pavan, D., Simões, P.I., Ernst, R., Fabre, A.C., 2021. Species diversity and biogeography of an ancient frog clade from the Guiana Shield (Anura: Microhylidae: *Adelastes, Otophryne, Synapturanus*) exhibiting spectacular phenotypic diversification. B.J.L.S. laa204 doi:10.1093/biolinnean/blaa204.

Fouquet, A., Martinez, Q., Courtois, E.A., Dewynter, M., Pineau, K., Gaucher, P., Blanc, M., Marty, C., Kok, P.J.R., 2013. A new species of the genus *Pristimantis* (Amphibia, Craugastoridae) associated with the moderately elevated massifs of French Guiana. Zootaxa 3750, 569–586.

Fouquet, A., Martinez, Q., Zeidler, L., Courtois, E.A., Gaucher, P., Blanc, M., Lima, J.D., Souza, S.M., Rodrigues, M.T., Kok, P.J.R., 2016. Cryptic diversity in the *Hypsiboas semilineatus* species group (Amphibia, Anura) with the description of a new species from the eastern Guiana Shield. Zootaxa 4084, 79–104.

D.R. FrostAmphibian species of the world: an online reference. Version 6.1 (01 january 2021)Electronic Database accessible athttps://amphibiansoftheworld.amnh.org/index.php2021American Museum of Natural History, New York, USA. doi.org/10.5531/db.vz.0001

Gehara, M., Crawford, A.J., Orrico, V.G., Rodríguez, A., Lötters, S., Fouquet, A., Barreintos, L.S., Brusquetti, F., De la Riva, I., Ernst, R., Gagliardi-Urrutia, G., Glaw, F., Guayasamin, J.M., Hölting, M., Jansen, M., Kok, P.J.R., Kwet, A., Lingnau, R., Lyra, M., Moravec, J., Pombal, J.P., Jr., Rojas-Runjaic, F.J.M., Schulze, A., Señaris, J.C., Solé, M., Rodrigues, M.T., Twomey, E., Haddad, C.F.B., Vences, M., Köhler, J., 2014. High levels of diversity uncovered in a widespread nominal taxon: continental phylogeography of the Neotropical tree frog *Dendropsophus minutus*. PloS One 9, e103958.

Gosner, K.L., 1960. A simplified table for staging anuran embryos and larvae with notes on identification. Herpetologica 16, 183–190.

Guayasamin, J.M., Castroviejo-Fisher, S., Trueb, L., Ayarzagüena, J., Rada, M., Vila, C., 2009. Phylogenetic systematics of Glassfrogs (Amphibia: Centrolenidae) and their sister taxon *Allophryne ruthveni*. Zootaxa 2100, 1–97.

IUCNThe IUCN red list of threatened species. Version 2020-3Downloaded on 10 March 2020https://www.iucnredlist.org2020

IUCNThe IUCN red list of threatened species. Version 2020-1Downloaded on [01 01 2020]https://www.iucnredlist.org2020

Jaramillo, A.F., De La Riva, I., Guayasamin, J.M., Chaparro, J.C., Gagliardi-Urrutia, G., Gutiérrez, R.C., Brcko, I., Vilà, C., Castroviejo-Fisher, S., 2020. Vastly underestimated species richness of Amazonian salamanders (Plethodontidae: *Bolitoglossa*) and implications about plethodontid diversification. Mol. Phylogenet. Evol. 149, 106841.

Keeffe, R., Blackburn, D.C., 2020. Comparative morphology of the humerus in forward-burrowing frogs. Biol. J. Linn. Soc. 131, 291–303.

Köhler, J., Jansen, M., Rodríguez, A., Kok, P.J.R., Toledo, L.F., Emmrich, M., Glaw, F., Haddad, C.F.B., Rödel, M.-O., Vences, M., 2017. The use of bioacoustics in anuran taxonomy: theory, terminology, methods and recommendations for best practice. Zootaxa 4251, 1–124.

Kok, P.J.R., Kalamandeen, M., 2008. Introduction to the taxonomy of the amphibians of Kaieteur national Park, Guyana. Abc Taxa 5, 1–278.

Kok, P.J.R., Russo, V.G., Ratz, S., Aubret, F., 2016. On the distribution and conservation of two "Lost World" tepui summit endemic frogs, *Stefania ginesi* Rivero, 1968 and *S. satelles* Señaris, Ayarzagüena, and Gorzula, 1997. Amphib. Reptile Conserv. 10, 5–12.

Kok, P.J.R., Russo, V.G., Ratz, S., Means, D.B., MacCulloch, R.D., Lathrop, A., Aubret, F., Bossuyt, F., 2017. Evolution in the south American "lost world": insights from multilocus phylogeography of stefanias (Anura, hemiphractidae, *stefania*). J. Biogeogr. 44, 170–181.

Kok, P.J.R., van der Velden, M., Means, D.B., Ratz, S., Josipovic, I., Boone, M., McDiarmid, R., 2020. Coping with the extremes: comparative osteology of the tepui-associated toad *Oreophrynella* and its bearing on the evolution of osteological novelties in the genus. Zool. J. Linn. Soc. 190, 114139.

Lima, A.P., Magnusson, W.E., Menin, M., Erdtmann, L.K., Rodrigues, D.J., Keller, C., Hödl, W., 2006. Guia de sapos da Reserva Adolpho Ducke, Amazônia Central. Editora INPA, Manaus.

Mendoza, E., Azizi, E., Moen, D.S., 2020. What explains vast differences in jumping power within a clade? Diversity, ecology and evolution of anuran jumping power. Funct. Ecol. 34, 1053–1063.

Menin, M., Rodrigues, D.J., Lima, A.P., 2007. Clutches, tadpoles and advertisement calls of *Synapturanus mirandaribeiroi* and *S.* cf. *salseri* in Central Amazonia, Brazil. Herpetol. J. 17, 86–91.

Menin, M., Waldez, F., Lima, A.P., 2008. Temporal variation in the abundance and number of species of frogs in 10,000 ha of a forest in central Amazonia, Brazil. South Am. J. Herpetol. 3, 68–81.

Neckel-Oliveira, S., Gordo, M., 2004. Anfíbios, lagartos e serpentes do Parque Nacional do Jaú. In: Borges, H.S., Iwanaga, S., Durigan, C.C., Pinheiro, M.R. (Eds.), Janelas para a Biodiversidade no Parque Nacional do Jaú: uma estratégia para o estudo da biodiversidade na Amazônia. Fundação Vitória Amazônica, Manaus, pp. 161–176.

Nelson, C.E., 1973. Systematics of the middle American upland populations of *hypopachus* (Anura: Microhylidae). Herpetologica 29, 6–17.

Nelson, C.E., Lescure, J., 1975. The taxonomy and distribution of *myersiella* and *Synapturanus* (Anura: Microhylidae). Herpetologica 31, 389–397.

Ouboter, P.E., Jairam, R., 2012. Amphibians of Suriname. Brill, Leiden, p. 376.

Peloso, P.L.V., Sturaro, M.J., Forlani, M., Motta, A.P., Gaucher, P., Wheeler, W.C., 2014. Phylogeny, taxonomic revision, and character evolution of the genera *Chiasmocleis* and *Syncope* (Anura, Microhylidae) in Amazonia, with descriptions of three new species. Bull. Am. Mus. Nat. Hist. 386, 1–96.

Peloso, P.L.V., Frost, D.R., Richards, S.J., Rodrigues, M.T., Donnellan, S., Matsui, M., Raxworthy, C.J., Biju, S.D., Lemmon, E.M., Lemmon, A.R., Wheeler, W.C., 2016. The impact of anchored phylogenomics and taxon sampling on phylogenetic inference in narrow-mouthed frogs (Anura, Microhylidae). Cladistics 32, 113–140.

Pyburn, W.F., 1975. A new species of microhylid frog of the genus *Synapturanus* from southeastern Colombia. Herpetologica 31, 439–443.
Pyburn, W.F., 1977. A new fossorial frog from the Colombian rainforest (Anura: Microhylidae). Herpetologica 32, 367–370 1976.
Rojas-Zamora, R.R., Fouquet, A., Ron, S.R., Hernández-Ruz, E.J., Melo-Sampaio, P.R., Chaparro, J.C., Vogt, R.C., de Carvalho, V.T., Pinheiro, L.C., Ávila, R.W., Farias, I.P., Gordo, M., Hrbek, T., 2018. A Pan-Amazonian species delimitation: high species diversity within the genus Amazophrynella (Anura: bufonidae). PeerJ 6 (e4941), 1–56.
Sanchiz, B., Tejedo, M., Sánchez-Herráiz, M.J., 2002. Osteological differentiation among iberian *Pelodytes* (Anura, Pelodytidae). Graellsia 58, 35–68.
Souza, M., 2019. História da Amazônia. Do período pré-Colombiano aos desafios do Século XXI. 391p. Record, Rio de Janeiro.
Thomas, K.N., Gower, D.J., Bell, R.C., Fujita, M.K., Schott, R.K., Streicher, J.W., 2020. Eye size and investment in frogs and toads correlate with adult habitat, activity pattern and breeding ecology. Proc. Royal Soc. B 287 (1935), 20201393.
Trueb, L., 1968. In: Cranial Osteology of the Hylid Frog, Smilisca Baudini, 18. University of Kansas Publications, Museum of Natural History, pp. 11–35.
Trueb, L., 1973. Bones, frogs, and evolution. In: Vial, J.L. (Ed.), Evolutionary Biology of the Anurans: Contemporary Research on Major Problems. University of Missouri Press, USA, pp. 65–132.
Vacher, J.-P., Kok, P.J.R., Rodrigues, M.T., Dias Lima, J., Lorenzini, A., Martinez, Q., Fallet, M., Courtois, E.A., Blanc, M., Gaucher, P., Dewynter, M., Jairam, R., Ouboter, P., Thébaud, C., Fouquet, A., 2017. Cryptic diversity in Amazonian frogs: integrative taxonomy of the genus *Anomaloglossus* (Amphibia: Anura: aromobatidae) reveals a unique case of diversification within the Guiana Shield. Mol. Phylogenet. Evol. 112, 158–173.
Vacher, J.-P., Chave, J., Ficetola, F.G., Sommeria-Klein, G., Tao, S., Thébaud, C., Blanc, M., Camacho, A., Cassimiro, J., Colston, T.J., Dewynter, M., Ernst, R., Gaucher, P., Gomes, J.O., Jairam, R., Kok, P.J.R., Lima, J.D., Martinez, Q., Marty, C., Noonan, B.P., Nunes, P.M.S., Ouboter, P., Recoder, R., Rodrigues, M.T., Snyder, A., Marques-Souza, S., Fouquet, A., 2020. Large scale DNA-based survey of frogs in Amazonia suggests a vast underestimation of species richness and endemism. J. Biogeogr. 47, 1781–1791.
Vieites, D.R., Wollenberg, K.C., Andreone, F., Köhler, J., Glaw, F., Vences, M., 2009. Vast underestimation of Madagascar's biodiversity evidenced by an integrative amphibian inventory. Proc. Natl. Acad. Sci. Unit. States Am. 106, 8267–8272.
Walker, C.F., 1973. In: A New Genus and Species of Microhylid Frog from Ecuador. Occasional Papers of the Museum of Natural History, 20. University of Kansas, pp. 1–7.
Wassersug, R., Pyburn, W.F., 1987. The biology of the Pe-ret toad, *Otophryne robusta* (Microhylidae), with special consideration of its fossorial larva and systematic relationships. Zool. J. Linn. Soc. 91, 137–169.
Zweifel, R.G., 1986. A new genus and species of microhylid frog from the Cerro de la Neblina region of Venezuela and a discussion of relationships among New World microhylid genera. Am. Mus. Novit. 2863, 1–24.